



REVIEW

Recent progress in sono-photodynamic cancer therapy: From developed new sensitizers to nanotechnology-based efficacy-enhancing strategies



Yilin Zheng^{a,†}, Jinxiang Ye^{b,†}, Ziying Li^a, Haijun Chen^{b,*}, Yu Gao^{a,b,*}

^aCancer Metastasis Alert and Prevention Center, College of Chemistry, Fuzhou University, Fuzhou 350116, China

^bFujian Provincial Key Laboratory of Cancer Metastasis Chemoprevention and Chemotherapy, Fuzhou University, Fuzhou 350116, China

Received 25 August 2020; received in revised form 27 September 2020; accepted 13 November 2020

KEY WORDS

Sensitizers;
Sonodynamic therapy;
Photodynamic therapy;
Sono-photodynamic therapy;
Nanoparticles;
Drug delivery;
Cancer;
Efficacy-enhancing strategies

Abstract Many sensitizers have not only photodynamic effects, but also sonodynamic effects. Therefore, the combination of sonodynamic therapy (SDT) and photodynamic therapy (PDT) using sensitizers for sono-photodynamic therapy (SPDT) provides alternative opportunities for clinical cancer therapy. Although significant advances have been made in synthesizing new sensitizers for SPDT, few of them are successfully applied in clinical settings. The anti-tumor effects of the sensitizers are restricted by the lack of tumor-targeting specificity, incapability in deep intratumoral delivery, and the deteriorating tumor microenvironment. The application of nanotechnology-based drug delivery systems (NDDSs) can solve the above shortcomings, thereby improving the SPDT efficacy. This review summarizes various sensitizers as sono/photosensitizers that can be further used in SPDT, and describes different strategies for enhancing tumor treatment by NDDSs, such as overcoming biological barriers, improving tumor-targeted delivery and intratumoral delivery, providing stimuli-responsive controlled-release characteristics, stimulating anti-tumor immunity, increasing oxygen supply, employing different therapeutic modalities, and combining diagnosis and treatment. The challenges and prospects for further development of intelligent sensitizers and translational NDDSs for SPDT are also discussed.

© 2021 Chinese Pharmaceutical Association and Institute of Materia Medica, Chinese Academy of Medical Sciences. Production and hosting by Elsevier B.V. This is an open access article under the CC BY-NC-ND license

(<http://creativecommons.org/licenses/by-nc-nd/4.0/>).

*Corresponding authors.

E-mail addresses: chenhaij@gmail.com (Haijun Chen), hellogaoyu@126.com (Yu Gao).

†These authors made equal contributions to this work.

Peer review under responsibility of Chinese Pharmaceutical Association and Institute of Materia Medica, Chinese Academy of Medical Sciences.

1. Introduction

Cancer is one of the leading causes of death in developed and developing regions of the world¹. As a complex disease, the uncontrolled cancer cells grow within different tissues, causing local damage and inflammation. Surgery, radiotherapy, and chemotherapy are traditional therapeutic approaches to treat and control the processes of this disease². However, they have some limitations, such as systemic toxicity, low selectivity, drug resistance, and potential long-term side effects. In order to overcome these shortcomings, various different types of therapies were developed, such as phototherapy, immunotherapy^{3–7}, gene therapy⁸, sono-dynamic therapy (SDT)⁹, and the combination of photodynamic therapy (PDT) and SDT (also known as sono-photodynamic therapy, SPDT)¹⁰.

As one of the available, safe, and minimally invasive treatment modalities based on the synergistic interactions of low-energy light and a photosensitizer, PDT has received widespread attention for the treatment of superficial tumors. Photosensitizers-mediated PDT activated by light can generate reactive oxygen species (ROS) to cause cell death. Over the past two decades, PDT has been developed as a promising tool to detect and treat cancer^{11,12}. However, one major disadvantage of PDT is the limited penetration of laser light into the deep tissues. This could be mitigated by shifting wavelengths into second near infrared (NIR-II) window. Sonosensitizers-mediated SDT with low-intensity ultrasound has better penetrability compared with NIR-II laser and could easily act on the tumor cells deep inside the biological tissues. The focused ultrasound energy to target deep tissue sites and the locally activation of the sonosensitizers-made SDT have improved treatment efficacy.

With the development of PDT and SDT in the past decade, many sensitizers were found to have not only photodynamic effects, but also sonodynamic anti-cancer effects. Therefore, SPDT has attracted tremendous interest for its enabling combination of SDT and PDT to obtain better therapeutic effects with reduced dose of both ultrasound/light energy and sensitizers, thus reducing the toxic side effects. Current sensitizers can be classified into organic, inorganic, and hybrid sensitizers for cancer therapy, but few of them are successfully applied in clinical settings. Most of the clinically used sensitizers lack tumor-targeting specificity, are incapable of deep intratumoral delivery, have skin phototoxicity, and tend to form aggregates in solution resulting in singlet oxygen (${}^1\text{O}_2$) production quenching. Besides, because of the oxygen (O_2) requirement during the PDT/SDT processes, the O_2 consumption might aggravate tumor hypoxia, thereby reducing the therapeutic effects.

Nanotechnology is the understanding of materials within the 1–100 nm size range and has been used in the design and development of drug delivery systems. Nanotechnology-based drug delivery systems (NDDSs) have achieved good effects in cancer treatment and can be used to improve the anti-tumor effect of drugs^{13–18}. NDDSs can improve targeting ability of sensitizers through targeted delivery to specific tumor cells or even specific organelles and enhance tumor penetration to increase intratumoral delivery, thus increasing the intracellular drug concentrations in cancer cells while reducing the toxic side effects on normal cells for effective SPDT. Some sensitizers loaded into NDDSs can achieve controlled drug release, prevent aggregation-caused ${}^1\text{O}_2$ quenching, and obtain triggered photoactivities. NDDSs could relieve tumor hypoxic microenvironment by increasing O_2 content in tumor tissues, and overcome the limitations of monotherapy by

integrating different therapies in a single formulation, thus improving the therapeutic effect of SPDT.

This review summarizes various sensitizers as sono/photosensitizers that can be further used in SPDT, and describes different strategies for enhanced SPDT by NDDSs. The challenges and prospects for further development of intelligent sensitizers and translational NDDSs for SPDT are also discussed.

2. Mechanisms of SPDT

PDT requires three basic conditions, namely light, O_2 , and photosensitizers. In the presence of light and O_2 , the photosensitizers that preferentially accumulate in the tumor site are activated to generate ROS (such as superoxide anion radicals O_2^- , hydroxyl radicals $\cdot\text{OH}$, hydrogen peroxides H_2O_2 , and ${}^1\text{O}_2$), resulting in cell death¹⁵. The photosensitizer under light irradiation can transit from the ground state to the single excited state, which then can transit to the excited triplet state through the intersystem crossing (ISC) process. The photosensitizer in excited triplet state may have two types of reactions¹⁹. It can directly react with substrate molecules to form free radicals, and then interact with O_2 to generate ROS (type I reaction), or can directly transfer its energy to ${}^3\text{O}_2$ (ground-state molecular O_2) to form ${}^1\text{O}_2$ (type II reaction)²⁰. The activated photosensitizer at the tumor site can damage tumor cells, resulting in necrosis, apoptosis, or autophagy²¹. In the blood vessel, the activated photosensitizer can disrupt the vascular walls and hinder the blood flow to the tumor to cause tumor hypoxia. PDT can also cause the release of some toxic substances to destruct tumor cells and activate the immune response²².

Similar to PDT, SDT also requires three basic conditions, including ultrasound, O_2 , and sonosensitizers. In the presence of ultrasound and O_2 , the generation of ROS through the stimulated sonosensitizer and the ultrasound-activated cavitation effects can induce apoptosis, necrosis, and autophagy, thus ultimately contributing to tumor destruction^{23–25}. Acoustic cavitation can be divided into inertial cavitation and non-inertial cavitation, which is mainly composed of three stages including nucleation, growth, and collapse of bubbles^{9,26}. Inertial cavitation and non-inertial cavitation produce mechanical effects, while inertial cavitation leads to the formation of sonochemical species, including ${}^1\text{O}_2$ and free radicals⁹. The free radicals generated by ultrasound-activated sonosensitizers can react with the O_2 to form peroxy and alkoxyl radicals. These radicals can induce lipid peroxidation (LPO) and apoptosis, which eventually cause cell death²⁷.

Sensitizers can be activated by ultrasound and light to generate more ROS for SPDT against cancer²⁸. The combination of PDT and SDT can cause tumor necrosis from the surface to the base²⁹. Combined therapy can also inhibit cell migration, decrease mitochondrial membrane potential, and induce apoptosis and autophagy^{30,31}. Inhibition of cell migration capacity was observed in the combined group, accompanied by the declined cell adhesion, severe microfilament network collapse, and decreased expression of matrix metalloproteinase-9 (MMP-9)³². However, the detailed mechanism of SPDT remains unclear. Possible mechanisms of SPDT in cancer therapy are shown in Fig. 1.

3. Sensitizers for cancer therapy

Sono/photo sensitizers can exert therapeutic effects of SDT/PDT and may be further used in SPDT. The chemical structures of

organic sensitizers and schematic illustration of inorganic and hybrid sensitizers used in cancer therapy are shown in Figs. 2 and 3. The characteristic parameters of the sensitizers used in different tumor cells or animal models are summarized in Table 1^{28–67}.

3.1. Organic sensitizers

3.1.1. Hematoporphyrin (*Hp*)

Hp as a first-generation photosensitizer, has poor water solubility, poor light absorption, and long-enduring skin photosensitivity, which limit its application in PDT^{68,69}. *Hp* could be used as a sonosensitizer for effective cancer treatment³³, solving the problem of poor light tissue permeability. Pheophorbide a^{35,36}, photofrin^{37,38}, tetra-(4-aminophenyl) porphyrin (TAPP)^{70,71}, and meso-tetra(4-carboxyphenyl) porphine (TCPP)^{72,73} have been proven effective in PDT or SDT.

3.1.2. Hematoporphyrin monomethyl ether (HMME)

HMME as a second-generation porphyrin-related sensitizer, has been used for PDT and SDT with significant anti-cancer effects^{74,75}. Compared with the first-generation sensitizers, HMME has several advantages including better solubility, rapid clearance in the body, and low toxicity⁷⁶. HMME-mediated SPDT achieved a significant better synergistic effect on rat C6 glioma cells than SDT or PDT alone. Further mechanism investigation showed that HMME-mediated SPDT induced Caspases 3, 8, and 9 activation through ROS generation³⁹. Despite the lack of *in vivo* study to verify its potential treatment effectiveness, recent results suggested that HMME-mediated SPDT could be a promising approach for human cancer therapy.

3.1.3. PH-1126

PH-1126, a pheophorbide a derivative, has been developed as a photosensitizer by Hamari Chemical Company. PH-1126 could generate more yield of $^1\text{O}_2$ than photofrin⁷⁷. In transplantable mouse squamous cell carcinoma (SCC) model, PH-1126-mediated photo-sonodynamic therapy (PSDT) produced stronger inhibition in tumor growth (98%) than PDT (76%) or SDT (43%) treatment alone. The combined approach could significantly improve the survival of mice as well as reduce drug dosage, resulting in reduced risk of potential skin

photosensitivity. Notably, the depth of necrosis increased more than 2-fold by adding of SDT, showing the promise for destruction of non-superficial or nodular tumors²⁹.

3.1.4. ATX-70

ATX-70 is a gallium-porphyrin derivative commonly used as a sonosensitizer⁷⁸. After intravenous administration of ATX-70 to mouse bearing colon 26 tumor at a dose of 2.5 mg/kg followed by ultrasound irradiation (3 W/cm²), the tumor size decreased within three days after the treatment. Another study reported that using ATX-70 as a sensitizer for PSDT significantly inhibited tumor growth (92%)²⁹.

3.1.5. *Sonoflora 1 (SF1)*

Chlorophyll is a group of fat-soluble magnesium porphyrin complex, and its derivatives have been used as photosensitizers in PDT^{79,80}. SF1 with molecular weight of 861.48 is a chlorophyll derivative. Using SF1 for SPDT in advanced breast carcinoma has been reported⁸¹.

3.1.6. Sonnelux-1

Sonnelux-1 with an average molecular weight of 942 is one of the chlorophyll analogs in that their backbone is porphyrin macrocyclic ring, and the center of the porphyrin ring is populated with a metal ion. This agent displayed high sonodynamic activity without obvious toxicity even in embryonic cells⁸². Initial *in vivo* studies showed that sonnelux-1-mediated SDT significantly suppressed the tumor growth of S-180 sarcoma xenograft⁸³. Another work reported that sonnelux-1 has both sonodynamic and photodynamic activities for sono-photodynamic cancer treatment⁸⁴.

3.1.7. Chlorin e6 (Ce6)

Ce6 is a naturally hydrophilic chlorin derivative, which is also considered to be a second-generation photosensitizer. Several studies demonstrated that Ce6 displayed significant photodynamic and sonodynamic anti-cancer effects. Recently, the combination of PDT with SDT by using Ce6 has been developed for cancer therapy. Ce6 was mainly localized in the mitochondria of the 4T1 murine breast cancer cells, and the enhanced cell death after SDT and PDT revealed the therapeutic potential of Ce6-mediated

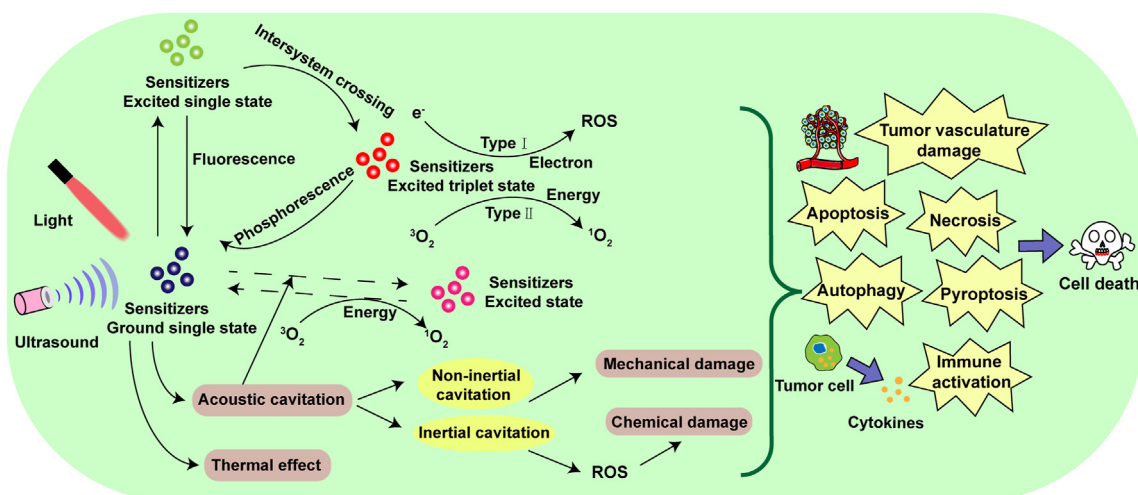


Figure 1 Possible mechanisms of SPDT in cancer therapy.

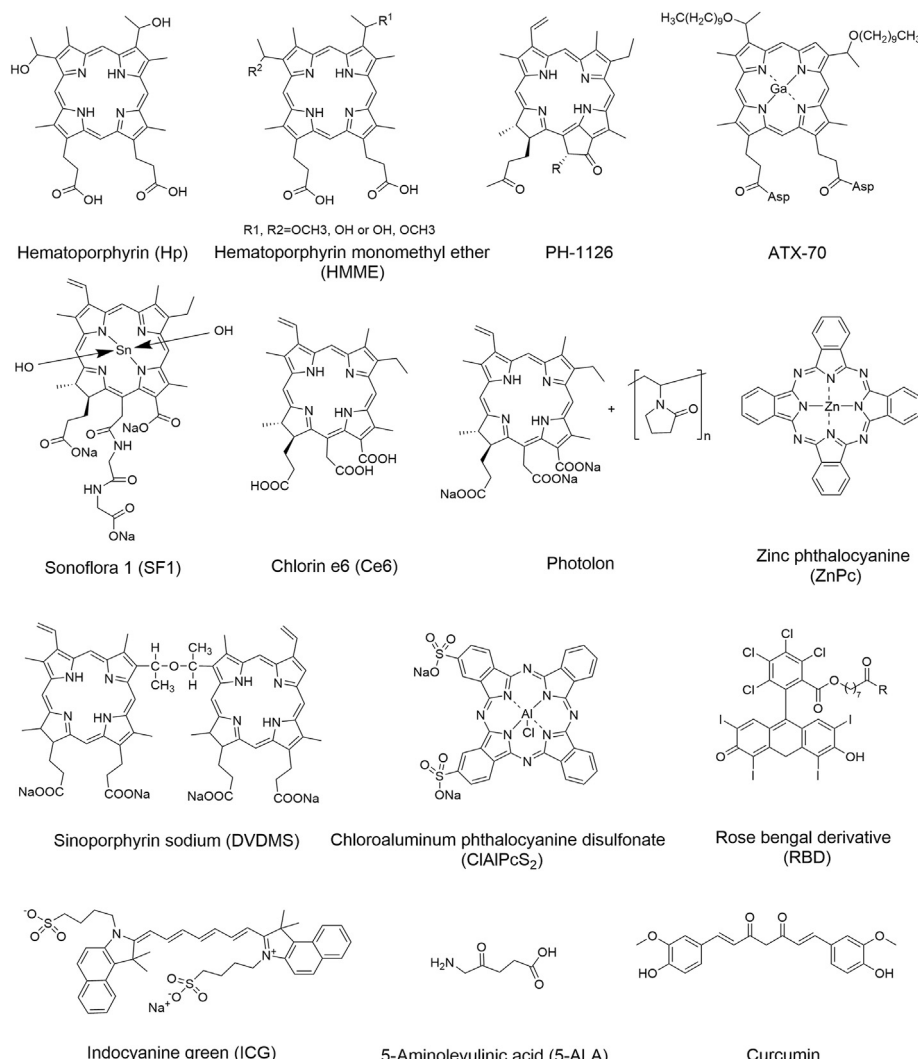


Figure 2 The chemical structures of organic sensitizers used in cancer therapy.

SPDT. Further investigations showed that Ce6-mediated SPDT could induce significant DNA damage and clonogenicity suppression³⁰. Additionally, ultrasound could enhance cell permeability, which in turn increases the uptake of Ce6 for subsequent laser irradiation, thus improving the therapeutic effect of SPDT^{30,40}. Ce6-mediated SPDT/PSDT decreased the cell viabilities in various breast cancer cell lines (MDA-MB-231, MCF-7, and 4T1) and Ce6-mediated SPDT markedly suppressed tumor growth and metastasis in 4T1 mouse breast cancer xenograft model. Besides, Ce6-mediated SPDT could cause mitochondrial membrane potential loss, induce tumor cell apoptosis, and decrease the expression levels of vascular endothelial growth factor (VEGF) and MMP-9⁴¹. The inhibition of the adhesion and migration was observed in MDA-MB-231 cells via Ce6-mediated SPDT or PSDT³². Another study investigated the underlying mechanisms of Ce6-mediated SPDT on apoptosis and autophagy in 4T1 cancer cells. SPDT could increase apoptosis-related protein Cleaved-Caspase-3 and PARP, decrease BCL-2 level, and maintain a stable BAX expression level. The conversion of LC3-I to LC3-II indicated the occurrence of autophagy, which was accompanied by the increased BECLIN-1 expression³¹.

Photolon is one of the most promising photosensitizers, which has been approved for clinical use. It is formed by the combination of Ce6 with hydrophilic polyvinylpyrrolidone (PVP) for improvement of aqueous solubility⁸⁵. Photolon is mainly distributed in the cytoplasmic organelles and nucleus after administration in the murine colon carcinoma CT-26 cells. Under the light dose of 1 J/cm², cell apoptosis reached 80%⁸⁶. Photolon can also increase the cytotoxic effect against glioma C6 cells under ultrasound irradiation⁸⁷. After intravenous administration of photolon to mouse bearing glioma C6 brain tumor at a dose of 2.5 mg/kg followed by ultrasound and laser irradiation treatment, tumor necrosis could be found in almost the entire tumor area⁴². These encouraging results demonstrated the potential clinical application of photolon-mediated SPDT.

3.1.8. *Sinoporphyrin sodium (DVDMS)*

DVDMS as a newly discovered photosensitizer is a conjugate of two porphyrin monomers with enhanced effects and low side effects compared to clinically used photofrin⁸⁸. Both *in vitro* and *in vivo* phototoxicity and sonotoxicity studies revealed that the DVDMS-mediated SPDT had stronger therapeutic effects on

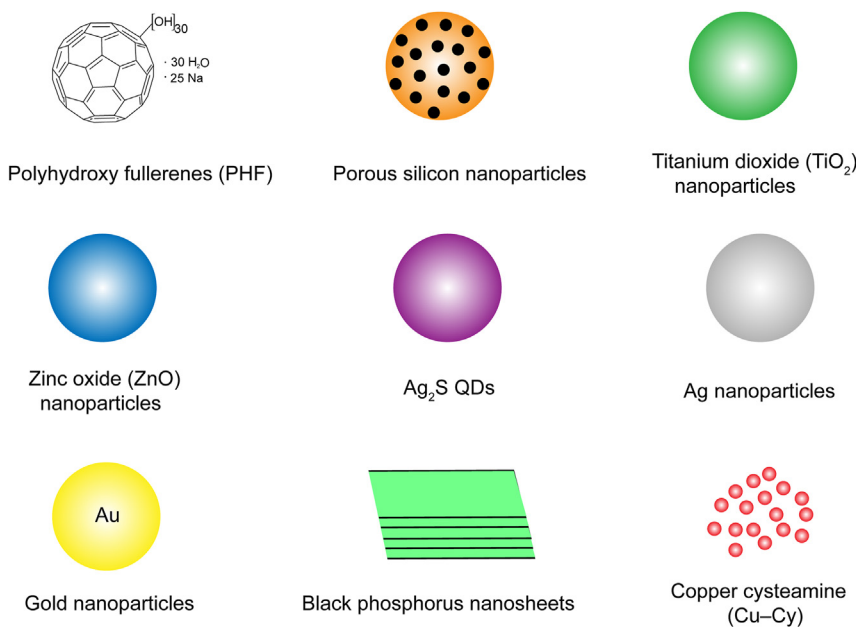


Figure 3 Schematic illustration of inorganic and hybrid sensitizers that have been synthesized for SPDT.

breast cancer over SDT or PDT alone⁴³. After the SPDT treatment, the cell viability losses in 4T1, MDA-MB-231, and MCF-7 cells were 77.48%–86.13%, and the tumor growth was significantly suppressed in a mouse 4T1 xenograft model. Investigations also revealed that DVDMS-mediated PSDT had equal anti-tumor effects when the order of SDT and PDT was exchanged.

3.1.9. Zinc (II) phthalocyanine (ZnPc)

Phthalocyanines as second generation photosensitizers, are aromatic heterocycles that consist of four isoindole rings bridged by nitrogen atoms, which have long absorption wavelength and high extinction coefficients⁸⁹. ZnPc is a phthalocyanine in which Zn metal ions are in the coordination center of the phthalocyanine. The Zn metal ions can strongly affect the photochemical properties of ZnPc and make ZnPc an efficient 1O_2 generator. ZnPc has the advantages of high therapeutic efficacy and minimal skin photosensitivity, and the generated ROS under light irradiation can damage tumor cells⁹⁰. However, ZnPc as a photosensitizer has not been approved for clinical use. ZnPc can be used as a sonosensitizer for SDT to produce radicals and damage cell membrane⁹¹. Studies on colon carcinoma tumor in BALB/c mice revealed that liposomal ZnPc could enhance ultrasound- and light-caused tumor shrinkage after light (160 mW/cm^2 , 300 J/cm^2) and ultrasound (1.1 MHz , 1 W/cm^2 , 10 min) treatments⁴⁴. It is worth mentioning that the arrangement of PDT and SDT was an important factor affecting the efficacy of ZnPc-mediated SPDT. The findings suggested the potency of development of phthalocyanines for SPDT in future.

3.1.10. Chloroaluminum phthalocyanine disulfonate ($ClAlPcS_2$)

$ClAlPcS_2$ as a photosensitizer demonstrated more phototoxic effects on G361 melanoma cells and MCF-7 breast adenocarcinoma cells than on NIH3T3 mouse fibroblasts and B16 mouse melanoma cells⁹². The number of necrosis cells treated with $ClAlPcS_2$ at $100\text{ }\mu\text{mol/L}$ is higher than that of apoptotic cells after PDT⁴⁵. MCF-7 cells treated with $100\text{ }\mu\text{mol/L}$ $ClAlPcS_2$ and ultrasound

followed by light irradiation at an intensity of 2 mW/cm^2 could produce higher ROS, which indicated that ultrasound could enhance the photodynamic effect in breast cancer cells²⁸. A549 human lung cancer cells treated with $ClAlPcS_2$ -mediated SDT after PDT could generate more ROS compared with those treated with SDT followed by PDT, demonstrating the great effects of the irradiation sequence on $ClAlPcS_2$ -mediated SPDT⁴⁶.

3.1.11. Rose bengal derivatives (RBDs)

Rose bengal (RB) as a hydrophilic anionic sensitizer has attracted considerable attention in many years. Previous studies have shown that RB can be used as a photosensitizer or sonosensitizer for the treatment of non-melanoma and melanoma skin cancer⁴⁹, but poor tumor accumulation limited its further clinical application⁹³. The amphiphilic derivatives of RB (RBDs) were synthesized to improve the accumulation ability of RB in tumors with high partition coefficient^{93,94}. One of RBDs linked to a lipid microbubble showed increased 1O_2 quantum yield and enhanced cytotoxicity *in vitro*, and could suppress tumor growth *in vivo* upon SDT⁹⁵. Recently, a series of amphiphilic RBDs with enhanced SPDT effects have been developed. *In vitro* studies revealed that RBDs exhibited significant anti-cancer effects in HepG2 cells which were treated with $0.5\text{ }\mu\text{mol/L}$ of RBDs for 2 h and then exposed to ultrasound (1.0 MHz , 2 W/cm^2 , 3 min) and light ($\lambda > 500\text{ nm}$) for 30 min at a dose of 27 J/cm^2 ⁴⁷. These findings implied the potential use of amphiphilic RBDs as sensitizers for SPDT in future.

3.1.12. Indocyanine green (ICG)

ICG as a medical diagnostic agent has been approved by the U.S. Food and Drug Administration (FDA)⁹⁶. Many studies employed ICG derivatives as useful platforms for design of NIR fluorescent probes⁹⁷. Human gingival fibroblast (HGF) cells treated with ICG under NIR irradiation could induce significant expression of apoptosis-related gene *BAX*⁹⁸, indicating ICG a promising photosensitizer for PDT. ICG-mediated SPDT could

Table 1 The characteristic parameters of sensitizers used in different cancer cell or animal models.

Sensitizer	Ultrasound			Laser light		Cancer cell type	Species	Ref.
	Frequency (MHz)	Intensity (W/cm ²)	Time (min)	Laser wavelength (nm)	Light dose (J/cm ²)			
Hp	2.2	5	3	—	—	S180	ICR mice	33
	—	—	—	635	4.05	Fadu	—	34
Pheophorbide a	1.92	3	15	—	—	S180	Male ICR mice	36
	—	—	—	675 ± 3	90	MCF-7	Female BALB/c nude mice	35
Photofrin	1.0	0.5	2	—	—	U251	—	37
	—	—	—	630	50–350	RIF	Female C3H mice	38
HMME	1	0.5	1.5	630	20–240	C6	—	39
PH-1126	1.0	0.51	10	650	44	SCC	C3H/HeN mice	29
ATX-70	1.0	0.51	10	575	88	SCC	C3H/HeN mice	29
Ce6	1.0	0.36	1	650	1.2	4T1	—	30,31
	1.0	0.36	1	650	1.2/2.5	MDA-MB-231	—	32,40
	1.90	1.6	3	650	120	4T1	Female BALB/c mice	41
Photolon	1	0.4/0.7/1.0	10	661	50–100	C6	White random-bred rats	42
DVDMS	1.90	1.6	3	635	50	4T1	Female BALB/c mice	43
ZnPc	1.1	1	10	670 ± 20	300	CT26	BALB/c mice	44
ClAlPcS ₂	1	2	10	660	15	B16F0, NIH3T3	—	45
	1	2	10	635	10	MCF-7	—	28
	1	2	10	635	15	A549	—	46
RBDs	1.0	2.0	3	>500	27	HepG2	—	47
ICG	1	3.5	3	830	56.7	RIF-1	C3H/HeN mice	48
5-ALA	1	3.0	10	—	—	EMT6	Female BALB/c mice	50
	—	—	—	630 ± 15	40	A431	Female SCID mice	49
Curcumin	0.86	2	5–15	—	—	THP-1	—	52
	—	—	—	445	100	Me180	Female BALB/c nude mice	51
MB	2	0.24	0.5	—	—	S180	—	54
	—	—	—	660	1–6	W256	Female Wistar rats	53
HB	0.84	0.25	1	—	—	SGC7901, SGC7901/ADR	—	56
	—	—	—	463	9	HepG2	—	55
Porous silicon	0.88	0.5	10	—	—	Hep2	—	58
	—	—	—	458	15–60	HeLa, NIH 3T3	—	57
TiO ₂ nanoparticles	1	1.0	2	—	—	C32	BALB/c athymic nude mice	60
	—	—	—	365	5	U87-MG	Female BALB/c nude mice	59
Ag ₂ S QDs	1.0	1.5	5	—	—	C26	Male BALB/c mice	61
	—	—	—	808	600	4T1	Female BALB/c mice	62
Ag nanoparticles	1	0.5–2	10	—	—	A2780	—	63
	—	—	—	—	5 × 10 ⁻⁴	MCF-7	—	64
Au nanoparticles	1.1	2	3	560	35	CT26	Male BALB/c mice	65
Black phosphorus	1	1.5	10	—	—	4T1	BALB/c nude mice	67
	—	—	—	660	0.6	MDA-MB-231	BALB/ <i>nu</i> – <i>nu</i> nude mice	66

Hp, hematoporphyrin; HMME, hematoporphyrin monomethyl ether; Ce6, chlorin e6; DVDMS, sinoporphyrin sodium; ZnPc, zinc (II) phthalocyanine; ClAlPcS₂, chloroaluminum phthalocyanine disulfonate; RBDs, rose bengal derivatives; ICG, indocyanine green; 5-ALA, 5-aminolevulinic acid; MB, methylene blue; HB, hypocrellin B; TiO₂, titanium dioxide; S180, mouse sarcoma; ICR, Institute of Cancer Research; Fadu, human oral cancer; MCF-7, human breast cancer; U251, human glioma; RIF, mouse radiation-induced fibrosarcoma; C6, rat glioma; SCC, human squamous cell carcinoma; 4T1, mouse breast cancer; MDA-MB-231, human breast cancer; CT26, mouse colon cancer; B16F0, mouse melanoma; NIH3T3, mouse fibroblast; A549, human non-small cell lung cancer; HepG2, human hepatocellular carcinoma; SCID, severe combined immunodeficient; EMT6, mouse mammary carcinoma; A431, human squamous cell carcinoma; THP-1, human monocytes; Me180, human cervical epidermoid carcinoma; W256, Walker 256 carcinosarcoma; SGC7901, human gastric adenocarcinoma; Hep2, human laryngeal cancer; HeLa, human cervical cancer; C32, human melanoma; U87-MG, human glioma; A2780, human ovarian carcinoma; —, not applicable.

lead to a 75% decrease in RIF-1 (radiation-induced fibrosarcoma) cells and the RIF-1 tumor volumes in C3H/HeN mice regressed to nearly immeasurable sizes at earlier stages. *In vivo* studies also demonstrated that even at Day 25 the RIF-1 tumor sizes had not fully recovered to their initial volume. Although the precise mechanism of this combination treatment is unclear,

the ICG-mediated SPDT might be beneficial for cancer therapy⁴⁸.

3.1.13. 5-Aminolevulinic acid (5-ALA)

Protoporphyrin IX (PpIX) can be used as a photosensitizer or sonosensitizer for cancer therapy^{99,100}. 5-ALA is a metabolic

precursor of the endogenously formed sensitizer PpIX, and has significant anti-tumor effects toward mouse mammary EMT6 tumor cells *in vitro* and *in vivo* under ultrasound *via* causing mitochondrial oxidative damage⁵⁰. 5-ALA-mediated SDT could cause certain killing effects on pancreatic cancer cells through mitochondrial-dependent apoptosis¹⁰¹. 5-ALA-mediated PDT/SDT can induce a significant overexpression of pro-apoptotic gene *APAF1* in human fibrosarcoma (HT-1080) cells¹⁰². Another study demonstrated that 5-ALA-mediated PDT or SDT had good therapeutic effects in squamous cell carcinoma (A431) cells and A431 ectopic tumors in mice⁴⁹.

3.1.14. Curcumin

Curcumin is the main active ingredient of turmeric, and has various bioactivity including anti-tumor, anti-oxidation and anti-inflammatory effects¹⁰³. Recently, studies have found that curcumin can be used as a sensitizer in PDT and SDT^{51,52}. Curcumin has the characteristics of poor absorption, low toxicity, and rapid clearance with reduced skin photosensitivity and poor bioavailability¹⁰⁴. Human keratinocyte HaCaT cells treated with curcumin under the ultraviolet radiation b (UVB) irradiation could induce caspase-3 activation, thus leading to cell apoptosis¹⁰⁵. Curcumin-mediated SDT could efficiently inhibit cell growth, and induce apoptosis and mitochondrial autophagy to cause cell death^{106,107}.

Other sensitizers also have been proved to be effective in PDT or SDT including acridine orange (AO)^{108,109}, methylene blue (MB)^{53,54}, IR780^{110,111}, and hypocrellin B (HB)^{55,56}.

3.2. Inorganic sensitizers

3.2.1. Polyhydroxy fullerenes (PHF)

Fullerenes with large molar absorption coefficients and high triplet yields can be used as photosensitizers for cancer therapy¹¹². Many functionalized fullerenes (such as hydroxyl, carboxyl, and amino functional groups) were synthesized to increase hydrophilicity¹¹³. PHF with water solubility, biocompatibility, and biodegradability could generate $^1\text{O}_2$ for PDT under light¹¹⁴. PHF can also be used as a potential sonosensitizer for SDT to treat tumors. Sarcoma 180 cells treated with PHF under ultrasound (2 MHz, 6 W/cm²) could induce cell damage and lipid peroxidation¹¹⁵. In another study, PHF combined with ultrasound could inhibit colon 26 tumor growth in male BALB/c mice¹¹⁶.

3.2.2. Porous silicon

Porous silicon is made of a network of intersecting silicon nanocrystals separated by nanometer-sized pores, and the visible photoluminescence could be observed at room temperature^{117,118}. Previous studies have shown that porous silicon can be used as a photosensitizer to generate $^1\text{O}_2$ through energy transfer at room temperature using light of the entire visible range¹¹⁹. Human cervical cancer HeLa cells treated with porous silicon nanoparticles under white light irradiation (60 J/cm²) can cause more cell death than the control group⁵⁷. Porous silicon nanoparticles can also be used as a sonosensitizer for SDT. Treatment of laryngeal cancer Hep-2 cells with porous silicon nanoparticles upon ultrasound could effectively inhibit cell proliferation⁵⁸. The dextran-coated porous silicon nanoparticles showed significant anti-tumor effects *in vitro* and *in vivo* under ultrasound irradiation with frequencies of 1–3 MHz and intensities of 1–2 W/cm²²⁰.

3.2.3. Titanium dioxide (TiO_2)

TiO_2 with photocatalytic properties can be used as a photosensitizer for cancer therapy. TiO_2 nanoparticles could induce apoptosis and necrosis under UV irradiation, and significantly reduce the growth of gliomas⁵⁹. In addition to the use of TiO_2 nanoparticles for PDT, TiO_2 nanoparticles with sonocatalytic properties can also be used as sonosensitizers for SDT. Ultrasound irradiation of TiO_2 nanoparticles at different frequencies and intensities had different sonodynamic therapeutic effects, and the generated $\cdot\text{OH}$ could effectively inhibit the growth of HepG2 cancer cells¹²¹. Preliminary researches of TiO_2 nanoparticles-mediated SDT against melanoma tumors⁶⁰, hepatoma¹²², and oral squamous cell carcinoma¹²³ were investigated. To prolong *in vivo* circulation time, hydrophilic TiO_2 was developed¹²⁴.

3.2.4. Zinc oxide (ZnO)

ZnO nanoparticles with high stability, wide band gaps, and inherent photoluminescence properties could be used for biomedical and cancer applications¹²⁵. ZnO nanoparticles as photosensitizers could produce ROS under UV irradiation and induce caspase-dependent apoptosis to reduce cell viability of SMMC-7721 hepatocarcinoma cells¹²⁶. ZnO as a semiconductor sonosensitizer has a potential in sonodynamic cancer therapy. Amino-propyl group-functionalized ZnO nanocrystals could produce ROS under the pulsed ultrasound exposure¹²⁷. In another study, a defect-rich gadolinium (Gd) doped ZnO (D- $\text{ZnO}_{x:\text{Gd}}$) was developed for effective deep tumor sonodynamic eradication. D- $\text{ZnO}_{x:\text{Gd}}$ can produce more ROS than other sonosensitizers TCPP, TiO_2 , and ZnO under ultrasound¹²⁸.

3.2.5. Ag_2S quantum dots (QDs)

Semiconductor QDs have attracted increasing attention due to tunable band gaps, high molar extinction coefficients, sufficient photostability, and the ability to generate multiple electron–hole pairs¹²⁹. Ag_2S QDs could be used as either sonosensitizer or photosensitizer to generate ROS for PDT and SDT^{61,62}. Biocompatible Ag_2S QDs prepared using high-temperature pyrolysis method were modified with PEGylated phospholipids to form nanoparticles, which had photodynamic behavior under 808 nm NIR irradiation. In addition, the Ag_2S QDs could be covalently attached on the polydopamine (PDA) surface to produce stronger PDT effects by generating more ROS⁶².

3.2.6. Silver (Ag) nanoparticles

Ag nanoparticles have anti-inflammatory and anti-cancer activities, which can be applicable for biomedicine¹³⁰. Ag nanoparticles could inhibit cancer cells under either ultrasound or light irradiation. A significant decrease of cell viability of human ovarian carcinoma A2780 cells was observed after the treatment of Ag nanoparticles and ultrasound, indicating that Ag nanoparticles have potential to be used as sonosensitizers for SDT⁶³. Biosynthesized Ag nanoparticles could produce ROS under light irradiation from a solar simulator to induce cell apoptosis. Further investigations revealed that Ag nanoparticles-mediated PDT could dramatically increase the ratio of BAX/BCL-2 protein expression in MCF-7 cells⁶⁴.

3.2.7. Gold (Au) nanomaterials

Au nanomaterials including Au nanocages, Au nanorods, and Au nanoparticles have been used for PDT or SDT^{131,132}. Lipid-coated Au nanocages could efficiently kill HeLa cells *in vitro* and inhibit B16F0 melanoma tumor growth upon NIR laser¹³¹. In another

study, significant inhibition of tumor growth was observed in BALB/c mice bearing colon carcinoma tumors treated with Au nanoparticles under intense pulsed light and ultrasound⁶⁵. The findings suggested that Au nanomaterials can be used for SPDT in future.

3.2.8. Black phosphorus

Black phosphorus is a metal-free layered semiconductor that has the advantages of tunable layer-dependent bandgap, wide light absorption, good biodegradability and biocompatibility, which can be used for PDT and SDT to treat cancer^{66,67}. Ultrathin black phosphorus nanosheets with high quantum yield of $^1\text{O}_2$ generation under the entire visible light region could induce cell apoptosis, inhibit cell proliferation, and suppress tumor growth under light irradiation⁶⁶. Recently, black phosphorus nanosheets which were stable within the timeframe of ultrasound-exposure before degradation were developed for SDT⁶⁷. Under ultrasound, black phosphorus nanosheets could produce ROS to effectively inhibit cell proliferation, and inhibit tumor growth and metastasis in 4T1 tumor-bearing BALB/c mice.

3.3. Hybrid sensitizers

Copper cysteamine (Cu–Cy) complex as a new type of sensitizer could be activated by light to produce $^1\text{O}_2$ ¹³³. Cu–Cy nanoparticles could generate ROS upon UV light (360 nm) and microwave (2, 5, and 10 W), and were effective in killing KYSE-30 cancer cells at low concentration of Cu–Cy and low microwave power in a relatively short time¹³⁴. Cu–Cy nanoparticles could inhibit the proliferation of human colorectal cancer cells, induce apoptotic cell death, and decrease mitochondrial membrane potential under X-ray-induced PDT for deep cancer treatment¹³⁵. In another study, breast cancer cells (MCF-7, 4T1, and MDA-MB-231 cells) treated with Cu–Cy nanoparticles and ultrasound exposure showed cell destruction and cell apoptosis due to ROS generation. Cu–Cy nanoparticles under ultrasound could significantly inhibit tumor growth in 4T1 tumor-bearing mice, suggesting the potential use of Cu–Cy as a sonosensitizer for SDT¹³⁶.

4. Different strategies for enhanced SPDT by NDDSs

Despite SPDT can induce tumor cell death, the severe skin photosensitization caused by the long-enduring photoactivities of sensitizers and the limited penetration depth of light therapy in tumor tissues restrict the application of SPDT. In addition, sensitizers with short blood circulation time, poor tumor-targeting specificity, and incapability of deep intratumoral penetration significantly affect the therapeutic effect of SPDT. Moreover, due to the O_2 dependence, the therapeutic efficacy of PDT/SDT in tumor hypoxic microenvironment is limited.

The fluorescence of sensitizer could be quenched inside the NDDSs and be recovered in response to the stimuli, thus reducing the skin photosensitization¹³⁷. The blood circulation time of sensitizers could be prolonged when entrapped in NDDSs, achieving high drug accumulation in tumor sites¹³⁸. NDDSs with targeting ligand-modification can improve tumor targeting and increase cellular uptake of sensitizers¹³⁹. NDDSs can also be designed to enhance intratumoral penetration of sensitizers and to relieve tumor hypoxia by increasing intracellular O_2 content¹⁴⁰.

Various NDDSs, including lipid-based nanoparticles, polymer-based nanoparticles, protein-based nanoparticles, and inorganic-

based nanoparticles can be used to deliver sensitizers for SPDT to treat tumors. Some inorganic sensitizers can also be used as NDDSs for drug delivery and exert SDT/PDT effects at the same time. The processes of drug delivery to solid tumors can be summed into five critical steps, termed the CAPIR cascade: blood circulation, accumulation and penetration into the tumor, cellular internalization, and intracellular drug release¹⁴¹ (Fig. 4). NDDSs can improve the drug delivery in one or two steps in CAPIR cascade. Different strategies with the assistance of NDDSs, such as overcoming biological barriers, improving the targeting of sensitizers, increasing intratumoral delivery, providing stimulus-responsive controlled-release function, stimulating anti-tumor immunity, increasing O_2 supply, employing different therapeutic modalities, and combining diagnosis and treatment have been explored to enhance the therapeutic effect of SPDT (Table 2^{71,138,140,142–147} and Supporting Information Table S1).

4.1. Overcoming biological barriers

Various biological barriers, such as mucosal, blood–brain barrier (BBB), blood vessel–tumor barrier can hamper the drug delivery, thus limiting the effectiveness of cancer therapy. Some carrier materials were introduced to prepare NDDSs to overcome biological barriers to improve drug transport and delivery. Chitosan can significantly increase the mucosal lipid fluidity to enhance drug delivery across the mucosal layer. Ce6 was incorporated into ursodeoxycholic acid-conjugated chitosan through hydrophobic interaction to fabricate nanoparticles. The nanoparticles could increase the transport of drugs through the mucosal layer for enhanced PDT¹⁴⁸. Mechanical action can be used to temporarily open biological barriers. Gas-filled microbubbles can be used as effective adjuvants to enhance SDT by increasing membrane permeability through ultrasound targeted microbubble destruction (UTMD)¹⁴⁹. Microbubbles can expand and push/disrupt the endothelial lining in the brain under ultrasound, thus temporarily opening the BBB. UTMD could open the BBB to improve the delivery of iRGD-modified DVDMs liposomes to the brain, and the nanosized DVDMs could significantly suppress the orthotopically implanted C6 gliomas via ROS generation under low intensity ultrasound¹⁵⁰. RBD with self-assembling nature can encapsulate a fluorinated gas to fabricate RBD-microbubbles which could *in situ* convert into RBD-nanoparticles by UTMD. The temporarily induced high permeability of the capillary wall facilitated the cellular drug uptake and resulted in about 7.5 times higher drug accumulation at the tumor tissue than that of other treatment groups to produce high yields of $^1\text{O}_2$ for enhanced SDT¹⁵¹. Acoustic droplet vaporization (ADV) can also generate microbubbles, making the blood vessel–tumor barrier more permeable. IR780-based nanodroplets (IR780-NDs) could penetrate deeper tumor tissues due to the disruption of blood vessels and tissue erosion caused by ADV, and produce ROS to induce cell apoptosis under ultrasound irradiation for enhanced deep-penetration SDT¹⁵².

4.2. Improving tumor-targeted delivery

After free drugs entered the body, only a small part of them distributed in the lesion site, and some of them metabolized before they reached the lesion site, resulting in reduced efficacy and serious toxic side-effects. NDDSs can selectively deliver drugs to tumor site through negative and active targeting, and thus effectively increase the concentration of drugs in tumor. According to

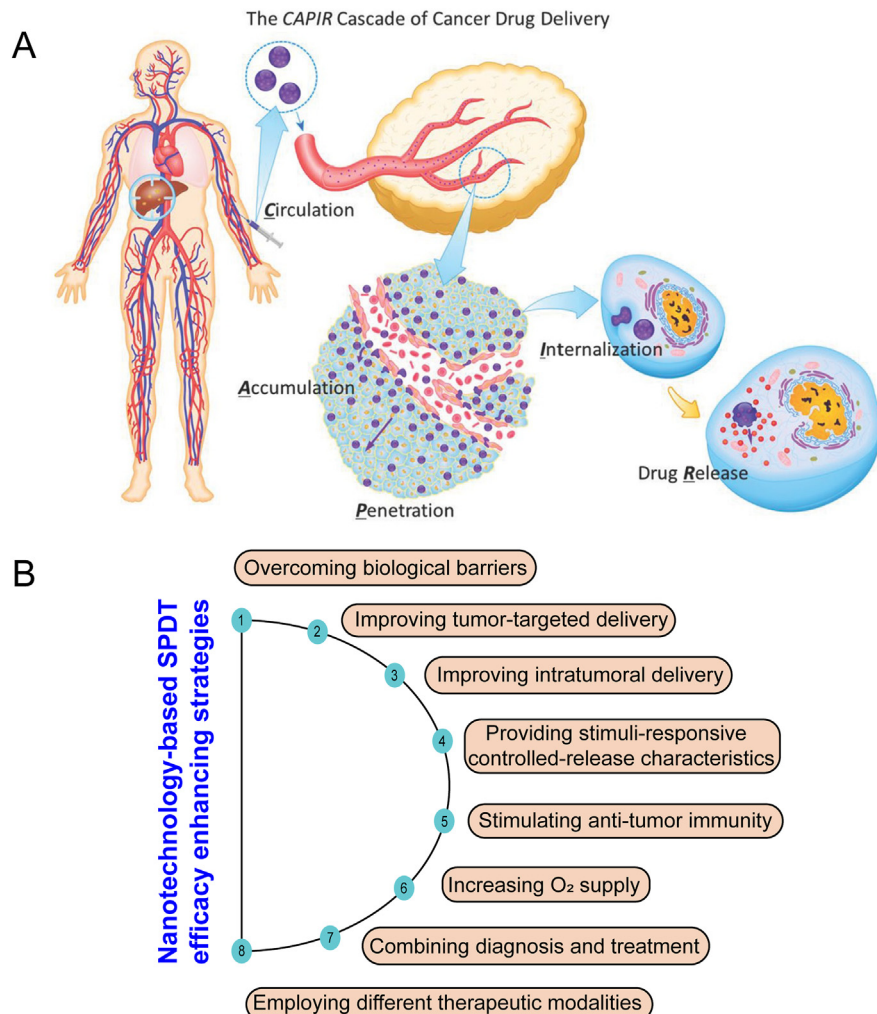


Figure 4 (A) Schematic diagram of the CAPIR cascade in cancer drug delivery: blood circulation, tumor accumulation and penetration, and subsequent cellular internalization and intracellular drug release. Reprinted with the permission from Ref. 141. Copyright © 2014, Wiley (B) Schematic illustration of different strategies to enhance SPDT by NDDSs for cancer therapy.

the different target sites, targeting can be divided into tissue/organ level, cellular level, and subcellular level.

4.2.1. Tumor tissue targeting

NDDSs can passively accumulate in tumor tissues due to the enhanced permeability and retention (EPR) effect. Chitosan/RBD composite nanoparticles with high drug accumulation in the tumor site were observed in CT-26 colon cancer transplanted BALB/c mice, which could be an efficient delivery system for targeted PDT⁹⁴. Some NDDSs with longer blood circulation time can also increase the distribution of sensitizers in tumor tissues. IPH@RBC composed of red blood cell (RBC) membranes and albumin nanoparticles (IPH) was used to encapsulate ICG and perfluorotributylamine (PFTBA). The elimination half-life ($t_{1/2}$) of IPH@RBC was about 15.71 h, which was nearly 14-fold higher than that of other treatment groups. IPH@RBC could significantly prolong blood circulation time and achieve 5.6-fold higher fluorescence of ICG in tumor site than that of ICG-HSA and IPH, thus effectively inhibiting tumor growth under NIR laser¹⁵³.

There are various factors and enzymes in tumor microenvironment. NDDSs can mediate the targeted delivery of the encapsulated sensitizers to the tumor site by recognizing these

factors and enzymes in the microenvironment. Matrix metalloproteinase-2 (MMP-2) is overexpressed in the tumor microenvironment. NDDSs modified by MMP-2-cleavable polypeptide could effectively reach the tumor site and responsively release cargoes inside the tumor tissue, thus improving the therapeutic effect. Au nanoparticles were co-modified with thiolated peptide HS-R8-PLGLAG-EK10 and 5-ALA to construct prodrug nanocarriers, which could effectively reach the tumor site by the mediation of MMP-2 for targeted PDT¹⁵⁴. In another work, MMP-2-cleavable polypeptide modified PEGylated Ce6 could self-assemble into nanoparticles to target tumor site with improved PDT¹⁵⁵.

4.2.2. Tumor cell targeting

Employing targeting ligands including folate (FA), transferrin, antibodies, aptamers which recognize receptors overexpressed on cancer cells could allow NDDSs achieving selective cancer cell targeting¹⁵⁶. NDDSs can be modified with targeting ligands to improve tumor cell targeting and drug delivery efficiency. FA-modified poly (lactic-co-glycolic) acid (PLGA) nanoplatforms could efficiently accumulate in tumor through FA receptor-binding and the loaded HMME could exert ultrasound-triggered

Table 2 Different NDDSs for enhanced SPDT.

NP Platform	Carrier material	Sensitizer	Light dose	Ultrasonic dose	Cancer cell type	Species	Function	Ref.
Polymeric NPs	PLGA/PFP/PTX	ICG	808 nm 1.5 W/cm ² , 5 min	1 MHz, 1 W/cm ² , 1 min	SKOV3	Female BALB/c athymic nude mice	O ₂ supply Combination therapy Integration of diagnosis and therapy	147
Micelles	C ₁₈ GR ₇ RGDS/ICG	ICG	808 nm 1.5 W/cm ² , 3 min	1 MHz, 2.4 W/cm ² , 5 min, 50% duty cycle	MDA-MB-231	Male nude mice	Intratumor delivery Combination therapy	144
Lipid-based NPs	DPPC/DPPG/DSPE-PEG-FA/ Cholesterol/PFH	ICG	808 nm 1.5 W/cm ² , 5 min	300 kHz, 1 W/cm ² , 30 s	SKOV3	Female BALB/c nude mice	Tumor-targeted delivery Combination therapy Integration of diagnosis and therapy	142
Protein-based NPs	HSA-Ce6/TAM	Ce6	660 nm 5 mW/cm ² , 30 min	—	4T1	Female nude mice	Intratumor delivery O ₂ supply	140
Peptide-based NPs	C ₁₈ GR ₇ RGDS/RB	RB	808 nm 1.5 W/cm ² , 3 min	1.0 MHz, 1.0 W/cm ² , 50%	HeLa	Male nude mice	Intratumoral delivery	143
Biomimetic NPs	RBC membrane/ CAuNCs/HA/ PXTK/dPPA	Pba	650 nm 270 mW/cm ² , 4 min	—	4T1	Female BALB/c mice	Intratumoral delivery Combination therapy	138
Inorganic NPs	HA-Mesoporous CaCO ₃	HMME	—	1 MHz, 1 W/cm ² , 1 min	MCF-7	BALB/c nude mice	Tumor-targeted delivery Stimuli-responsive release Integration of diagnosis and therapy	145
Metal-organic frameworks	LMWHA-PEI-MPB	HMME	—	3 MHz, 1.0 W/cm ² , 1 min	4T1	Female BALB/c mice	Immunity modulation O ₂ supply	146
Hybrid NPs	p-(OEOMA- <i>co</i> - MEMA)/Pt-CuS	TAPP	—	1 MHz, 1.0 W/cm ² , 5 min, 60% duty cycle	CT26	Female BALB/c mice	O ₂ supply Combination therapy Integration of diagnosis and therapy	71

NPs, nanoparticles; PLGA, poly(lactic-*co*-glycolic) acid; PFP, perfluoropentane; PTX, paclitaxel; ICG, indocyanine green; DPPC, dipalmitoylphosphatidylcholine; DPPG, 1,2-dipalmitoyl-*sn*-glycero-3-phospho-(1'-rac-glycerol); DSPE-PEG-FA, 1,2-distearoyl-*sn*-glycero-3-phosphoethanolamine-*N*-(folate(polyethyleneglycol)); PFH, perfluorohexane; HSA, human serum albumin; TAM, tamoxifen; Ce6, chlorin e6; RB, rose bengal; RBC, red blood cell; CAuNCs, cationized gold nanoclusters; HA, hyaluronic acid; PXTK, paclitaxel dimer prodrug; dPPA, anti-PD-L1 peptide; Pba, pheophorbide a; CaCO₃, calcium carbonate; HMME, hematoporphyrin monomethyl ether; LMWHA, low molecular weight hyaluronic acid; MPB, mesoporous Prussian blue; p-(OEOMA-*co*-MEMA), poly(oligo(ethylene oxide) methacrylate-*co*-2-(2-methoxyethoxy) ethyl methacrylate; CuS, copper sulfide; TAPP, tetra-(4-aminophenyl) porphyrin; SKOV3, human ovarian cancer; MDA-MB-231, human breast cancer; 4T1, mouse breast cancer; HeLa, human cervical cancer; MCF-7, human breast cancer; CT26, mouse colon cancer; —, not applicable.

SDT to suppress tumor growth in MDA-MB-231 tumor-bearing mice¹⁵⁷. AS1411 aptamer-modified upconversion nanoplatform could promote cellular uptake through nucleolin-binding and achieve NIR-triggered PDT to treat deep-seated tumors¹⁵⁸. TiO₂-coated upconversion nanoparticles (UCNPs) modified with PEGylated epithelial growth factor receptor (EGFR) affibody could specifically target EGFR expressing cancer cells and were internalized much more rapidly and efficiently (~3.8-fold) than unmodified TiO₂-UCNPs, significantly delaying tumor growth under 980 nm NIR-II laser irradiation¹⁵⁹.

FA-targeted perfluorohexane (PFH)/ICG-loaded lipid nanoparticles could specifically target SKOV3 ovarian cancer cells and be endocytosed with a remarkable efficiency for PSDT/photothermal therapy (PTT) treatment in ovarian tumors. The photo-acoustic (PA) signals in the tumor area could reach the maximal intensity at 6 h after injection of FA-modified nanoparticles, which is stronger than the non-FA-targeted group at 12 h post-injection¹⁴².

4.2.3. Cellular organelle targeting

Various intracellular organelles, including lysosomes, mitochondria, Golgi complex, endoplasmic reticulum, and nuclei, involved in the pathogenesis of cancer and sensitizers can exert their desired therapeutic effects in these organelles. Modification of NDDSs with specific moieties can deliver sensitizers to specific organelles for better efficacy. NDDSs modified with triphenylphosphonium (TPP) have been developed to actively target mitochondria. Mitochondria-targeted mesoporous silica nanoparticles (MSN) could generate a large amount of ROS under laser irradiation and boost the Ce6-mediated PDT, thus causing the mitochondrial dysfunction and irreversible cell death¹⁶⁰. Mitochondria-targeted HMME/Cu²⁺ ion-doped mesoporous silica nanosystems could generate ¹O₂ under ultrasound, and the released Cu²⁺ ions could convert endogenous H₂O₂ to ·OH, thus effectively inducing mitochondrial disintegration and damage¹⁶¹. A conjugate TAT-IR780 and doxorubicin (DOX) were self-assembled into TID nanoparticles for perinuclear region targeting. The TID nanoparticles-mediated PDT could generate ROS and induce cell apoptosis under 785 nm laser irradiation¹⁶².

4.2.4. Multi-targeting

NDDSs target more than one site could minimize off-target effects with high target specificity and selectivity. NDDSs designed with multiple-targeting effects can better accumulate in tumors, achieving better therapeutic effects. Receptor integrin not only overexpresses in tumor cells, but also participates in tumor angiogenesis. iRGD (CRGDKGPDC)-modified liposomes could target tumor vessels and tumor cells through integrin $\alpha_v\beta_3$ -binding, and could efficiently ablate laryngeal carcinoma Hep-2 cells upon phototherapy¹⁶³. In addition to iRGD peptide, F3 peptide that specifically targets nucleolin can also be used for mediating dual-targeting delivery. F3 peptide-modified nanoparticles were developed for targeted delivery to both tumor cells and tumor angiogenic endothelial cells to exert SDT effects *in vitro* under ultrasound¹⁶⁴. Ce6-conjugated β -cyclodextrin and a designed peptide Ad-CGKRK-GFLG-EE-HAIYPRH (T7) could self-assemble into supramolecular micelles with dual targeting ability for enhanced PDT. The micelles could enhance intracellular internalization *via* a transferrin receptor (TfR)-mediated pathway, and could accumulate in the mitochondria due to the exposure of CGKRK to prompt ROS generation upon irradiation¹⁶⁵.

4.3. Improving intratumoral delivery

Although some drugs can reach the tumor sites, they cannot get into deep tumor tissues to obtain good therapeutic effects. Solid tumors are characterized by abnormal tumor vasculature, increased interstitial fluid pressure, as well as dense extracellular matrix (ECM). The deep tumor penetration depends on the physiology of tumors and the properties of NDDSs. Particle size, surface charge, and particle shape of NDDSs have impacts on tumor penetration¹⁴. NDDSs with suitable physiochemical properties can penetrate into the internal area of the tumor and reach intratumoral cancer cells to enhance the anti-tumor effect.

4.3.1. Size transition

Nanoparticles with large size have a good retention ability in tumor tissues, while nanoparticles with smaller sizes are apt to penetrate deeply into tumor sites¹⁶⁶. Size-switchable NDDSs with self-destructive and tumor penetration characteristics have been developed for enhanced cancer therapy. Biomimetic nanoparticles with optimal size composed of RBC membrane, hyaluronic acid (HA), and cationized Au nanoclusters could degrade into small cores in the presence of hyaluronidase to enhance tumor penetration, and exhibit high tumor accumulation for chemotherapy/PDT/immunotherapy. RBC membrane-coated nanoparticles with the sizes of 300, 200, and 150 nm, showed significantly much higher internalization than the uncoated groups at 4 h (increased by 2.02-, 1.55- and 1.95-fold)¹³⁸. The self-assembled human serum albumin (HSA)-Ce6/tamoxifen nanocomplexes could change particle size from about 130 to 10 nm owing to the protonation of tamoxifen to induce pH-responsive dissociation of HSA-Ce6. The size change of the nanocomplexes could significantly improve intratumoral penetration for enhanced PDT¹⁴⁰. A hypoxia-responsive human serum albumin (HSA)-based nanosystem was developed with a size of 100–150 nm under normoxic condition. The nanosystem could quickly dissociate into ultrasmall therapeutic nanoparticles (below 10 nm) under the hypoxic tumor microenvironment to enhance intratumoral penetration and improve PDT effects¹⁶⁷. ICG-conjugated poly (amidoamine) dendrimer (PAMAM-ICG) was conjugated to PEG-*b*-poly (ϵ -caprolactone) (PEG-*b*-PCL) through a ¹O₂-responsive thioketal bond. The drug-conjugated copolymer/Ce6 nanoparticles could accumulate in the blood vessel extravasation sites due to their large size. Upon 660 nm irradiation, the activated Ce6 could generate ¹O₂ to kill cancer cells in the perivascular and small-sized PAMAM-ICG was simultaneously released due to the cleavage of the thioketal bond to penetrate into the internal area of the tumor. The released PAMAM-ICG could efficiently ablate cancer cells in the hypoxic microenvironment after 808 nm irradiation¹⁶⁸.

4.3.2. Charge reversal

Besides particle size, surface charge also has great effects on the tumor permeability and treatment efficacy of NDDSs. Because positively charged NDDSs can easily enter negatively charged cells, nanoparticles can be designed to be transformed into positively charged particles *via* pH-induced surface charge switching to penetrate into tumor cells^{169,170}. Hollow silicon nanoparticles with catalase within their inner cavities and Ce6 doped in the silica lattice structure were modified with (3-carboxypropyl) triphenylphosphonium bromide and a pH-responsive charge-convertible polymer. The nanoparticles could convert into

positively charged nanoparticles under acidic condition (pH 6.8) for enhanced tumor penetration and improved PDT¹⁷⁰.

4.3.3. Membrane transport

Some membrane transport peptides can traverse the cell membrane for drug delivery. A peptide amphiphile ($C_{18}GR_7RGDS$) was synthesized by introducing a hydrophilic (RGDS) terminal and a hydrophobic (C_{18}) terminal into the spacer ends of a cell-penetrating chain of R_8 . The mixture of RB and $C_{18}GR_7RGDS$ could self-assemble into nanocapsules with cell-penetrating properties to inhibit HeLa tumor growth upon PSDT treatments¹⁴³. Peptide amphiphile $C_{18}GR_7RGDS$ and ICG could self-assemble into functional nanomicelles with efficient cell-penetrating capabilities, which could significantly inhibit MDA-MB-231 tumor growth after PSDT/PTT treatments¹⁴⁴ (Fig. 5).

4.4. Providing stimuli-responsive controlled-release characteristics

NDDSs can be designed to be responsive to external or intracellular environment to achieve controlled release of sensitizers. Stimuli-responsive release of NDDSs can avoid premature drug release and enhance the intracellular concentration of drugs in cancer cells. The multiple stimuli-responsive NDDSs may enable precise drug release, thus ultimately improving the therapeutic effect. In addition, NDDSs with stimuli-responsive release character can overcome the limitations of sensitizers including phototoxicity and aggregation-caused quenching.

4.4.1. External environment-responsive release

NDDSs can be designed to trigger drug release in responsive to external stimuli, including ultrasound, light, and light-induced heat. DVDMs-encapsulated liposome–microbubble complexes could be triggered to release DVDMs through ultrasound-induced

cavitation, and enhance SDT against breast cancer¹⁷¹. ICG was loaded into reconstituted high density lipoproteins (rHDL) to achieve controlled release of ICG and produce 1O_2 for PDT under 808 nm laser irradiation¹⁷². ZnPc and Au nanoparticles were incorporated into liposomes. Light-induced heat could enhance the liquidity of liposomal membrane to promote the instantaneous release of ZnPc (80% after 72 h) for phototherapy¹⁷³. DOX and Ce6-loaded hollow mesoporous copper sulfide (CuS) nanoparticles were co-loaded with a phase change material 1-tetradecanol. Under 808 nm light irradiation, 1-tetradecanol was melted to trigger Ce6 release and the PDT effects were then activated under 660 nm¹⁷⁴.

4.4.2. Intracellular environment-responsive release

The low pH, hypoxia, and redox condition in tumor microenvironment, and the various enzymes in tumor-associated cells can be used to stimulate drug release. Some NDDSs containing glutathione (GSH)-sensitive materials could achieve the controlled release of sensitizers in redox environment. An amphiphilic branched copolymer with pendant vinyl groups were synthesized using polyethylene glycol (PEG) and ethylene glycol dimethacrylate (EGDMA). The copolymer/Ce6 self-assembled micelles could react with GSH to release Ce6 through swelling of the micelles and decrease the level of GSH for enhanced PDT¹⁷⁵. NDDSs containing redox-cleavable disulfide bonds can be designed to trigger sensitizer release in GSH rich tumor-specific environment. The conjugation of pheophorbide a and alginate with redox-sensitive disulfide linkages was used to load DOX to fabricate a nanosystem, which could accelerate approximately 90% pheophorbide a release at high GSH level (10 mmol/L) for PDT against B16 tumor cells¹⁷⁶.

Sensitizers in NDDSs could be triggered to be released by breaking pH-sensitive covalent linkages under acidic environment. D- α -Tocopheryl polyethylene glycol 1000 succinate (TPGS) was

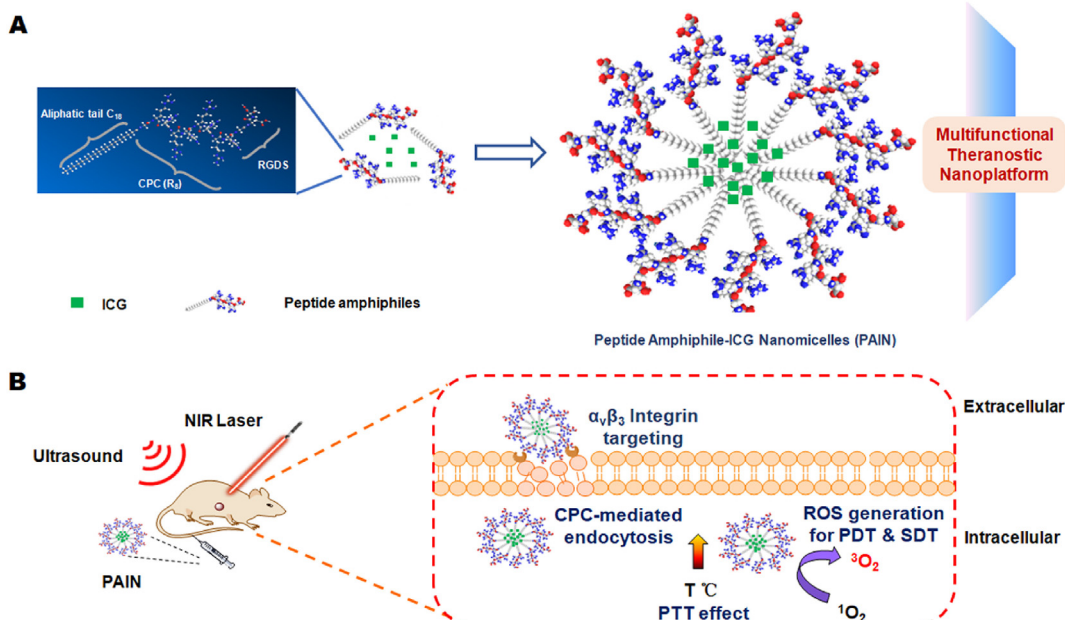


Figure 5 A schematic illustration for the chemical structure of peptide amphiphile-ICG nanomicelles (PAIN) to treat breast cancer. PAIN with efficient cell-penetrating capabilities could penetrate into tumor cells for synergistic SDT/PDT/PTT. Reprinted with the permission from Ref. 144. Copyright © 2020, Elsevier, Ltd.

conjugated to acid-sensitive *cis*-aconitic anhydride-modified DOX to form prodrug nanoparticles. The prodrug nanoparticles encapsulated with Ce6 could be triggered to release Ce6 at pH 5.5 due to the hydrolysis of the acid-sensitive amide linker for PDT¹⁷⁷. In another work, 5-ALA was encapsulated in a core–shell structured nanoparticle containing a pH-sensitive hydrazone bond for pH-responsive release for PDT¹⁷⁸. Besides, the fabrication of NDDSs through pH-sensitive noncovalent interactions (such as hydrogen bonding, host-guest and electrostatic interactions) has been developed for controlled drug release under acidic condition. Chitosan and catalase can fabricate micelles through electrostatic interaction. The micelles loading Ce6 were disassembled in acidic environment to trigger the release of Ce6 for effective PDT¹⁷⁹. Furthermore, some pH-sensitive materials can be employed to prepare NDDSs to facilitate controlled release of drugs under acidic tumor microenvironment. A lipid bilayer-coated calcium carbonate (CaCO_3) nanoparticles as a pH-responsive nanoplatform could be decomposed into Ca^{2+} and carbon dioxide (CO_2) under acidic condition to trigger the release of Mn^{2+} -chelated Ce6 for PDT¹⁸⁰. Chitosan-capped biodegradable hollow mesoporous silica nanoparticle were developed to trigger the release of pheophorbide a (increased to 68.9% of drug release at 48 h) for PDT under low pH via pH-dependent swelling effect of the coating layer¹⁸¹.

4.4.3. Multiple stimuli-responsive release

NDDSs can be designed to release sensitizers in response to double stimuli or triple stimuli to obtain precise drug release. A pH/ultrasound dual-responsive nanoplatform HMME/ CaCO_3 -HA, which was HMME loaded HA-modified mesoporous CaCO_3 nanoparticles, could be decomposed under low pH and ultrasound. The release of HMME at pH 5.8 with ultrasound increased by 56.4% compare to that at pH 5.8 without ultrasound, which is 27.3% higher than that at pH 7.4 without ultrasound¹⁴⁵. A pH/light responsive nanoplatform composed of PEG, Hp, and DOX has been developed to trigger the release of Hp at pH 5.8 along with laser irradiation for PDT¹⁸². Curcumin-loaded mesoporous magnetic carbon nitride nanohybrids could be triggered to release curcumin for PDT at lysosomal pH 5.2 in the presence of an alternating current magnetic field¹⁸³. Enzyme/redox, pH/temperature, and pH/GSH dual stimuli-responsive nanoplatforms have been developed for controlled release of Ce6 to exert PDT effects^{184–186}. The mixture of nitroimidazole-modified chitosan and RBD could self-assemble into nanoparticles, which could be triggered to release drugs in response to intratumoral hypoxia and acidic environment for enhanced PDT¹⁸⁷. In another study, multi-triggered tumor-responsive drug delivery vehicles have been developed to promote the release of Ce6 under pH, GSH, and protease triple stimuli for enhanced PDT¹⁸⁸.

4.5. Stimulating anti-tumor immunity

Immunotherapy orchestrates the immune system to find and kill the residual tumor cells, thus reducing the risk of cancer metastasis and recurrence¹⁸⁹. Some nanomaterials, such as MnO_2 , UCNPs, and CaCO_3 can elicit immunogenic cell death (ICD) or activate macrophages for cancer treatment¹⁹⁰. PDT can also induce anti-tumor immune response by stimulating the immune system, further enhancing the anti-tumor effect¹⁹¹. NDDSs containing carrier materials which have the function of activating the immune system could work with the sensitizers to achieve a synergistic effect. HA polysaccharose with different molecular weights can produce pro-inflammatory mediators and modulate

macrophage phenotype. Low molecular weight HA-modified mesoporous Prussian blue nanoparticles loaded with HMME could not only remodel tumor-associated macrophages (TAMs) phenotype from pro-tumor M2 to anti-tumor M1, but also exert SDT effects under ultrasound irradiation, thus inhibiting the proliferation and metastasis of 4T1 tumors¹⁴⁶. PLGA was used to load perfluoropentane (PFP), ICG, and oxaliplatin (OXP) for combined PSDT/chemotherapy. The nanocomplexes could induce ICD accompanied by the release of damage-associated molecular patterns (DAMPs), such as calreticulin (CRT), adenosine-5'-triphosphate (ATP), and high-mobility group box 1 (HMGB1), and elicit stronger activity of cytotoxic T lymphocyte (CTL)¹⁹².

4.6. Increasing O_2 supply

The tumor microenvironment is a local homeostatic environment composed of different kinds of cells, such as cancer cells, endothelial cells, cancer-associated fibroblasts (CAFs), cancer stem cells (CSC), immune cells as well as ECM, which is often accompanied by hypoxia and low pH¹⁹³. Tumor hypoxic micro-environment can reduce the anti-tumor effects, impede immune cell infiltration of tumors, and accelerate tumor recurrence and metastasis¹⁹⁴. The continuous O_2 consumption in PDT/SDT might aggravate tumor hypoxia. NDDSs can be designed to supply O_2 , which can alleviate tumor hypoxia, thereby effectively enhancing the therapeutic effects.

4.6.1. Catalase catalyzed reaction

NDDSs containing catalase could decompose the endogenous H_2O_2 to generate O_2 for relieving hypoxia. TCPP-conjugated catalase through amide coupling was mixed with fluorinated chitosan (FCs) to form catalase-TCPP/FCs nanoparticles. The nanoparticles could greatly improve transmucosal adsorption and intratumoral penetration, and generate O_2 to relieve tumor hypoxia, thus achieving effective SDT tumor suppression⁷³. The mixture of fluorinated polyethylenimine (F-PEI) and Ce6-conjugated catalase was able to form self-assembled catalase-Ce6/F-PEI nanoparticles to effectively relieve tumor hypoxia and improve PDT to destruct orthotopic bladder tumors¹⁹⁵. RBC vesicles were used to encapsulate Pluronic F-127-modified Ag_2S QDs to form biomimetic nanoparticles. Oral administration of anti-tumor drug phenethyl isothiocyanate (PEITC) in mice increased the H_2O_2 concentration, and the enzyme in RBC membranes could catalyze H_2O_2 in tumor cells to alleviate hypoxia for enhanced SDT⁶¹.

4.6.2. Metal-based catalytic reactions

NDDSs containing Cu-based nanoagents¹⁹⁶, Prussian blue nanoparticles¹⁴⁶, Fe(OH)_3 nanocolloids¹⁹⁷, hollow iron oxide nanoparticles (HIONs)¹⁹⁸, manganese dioxide (MnO_2) nanoparticles¹⁹⁹, platinum (Pt) nanoparticles^{71,200}, and Au_2Pt nanozymes²⁰¹ with catalase-like activity could degrade H_2O_2 to O_2 to overcome tumor hypoxia. The mixture of HSA, potassium permanganate (KMnO_4), and Ce6 could self-assemble into HSA- MnO_2 -Ce6 nanoparticles to produce O_2 to improve the efficacy of PDT for orthotopic bladder cancer²⁰². The nanosystems Hp-HIONs@PDA-PEG composed of HIONs, Fe_3O_4 , Hp, PDA, and PEG could produce O_2 to dramatically enhance SDT efficacy, which could effectively suppress tumor growth (85.58%) after SDT/magnetic hyperthermal therapy treatments¹⁹⁸. Hollow semiconductor CuS, noble metallic Pt, a temperature-sensitive polymer (poly (oligo (ethylene oxide)methacrylate-*co*-2-(2-methoxyethoxy) ethyl methacrylate) [p-

(OEOMA-*co*-MEMA)], and TAPP were combined together to form Pt–CuS–P-TAPP nanoparticles. The nanoparticles could accelerate the catalytic activity of Pt to elevate the O₂ level under NIR irradiation-induced heat, and produce ROS to induce cell apoptosis under ultrasound⁷¹. Au₂Pt nanozymes were covalently linked with Ce6 through a PEG linker to form Au₂Pt-PEG-Ce6 nanoformulation. The nanoformulation possessed catalase-like activity and peroxidase-like activity to generate O₂ and ·OH for synergistic PTT, PDT, and chemodynamic therapy²⁰¹.

4.6.3. Employing O₂ carriers

Some O₂ carriers, such as PFTBA¹⁵³, perfluoroctyl bromide (PFOB)²⁰³, PFP¹⁴⁷, and PFH²⁰⁴ were entrapped into NDDSs to generate O₂ for relieving hypoxia. Fluorocarbon (FC)-chain-functionalized hollow mesoporous organosilica nanoparticles carrying IR780 could supply enough O₂ to solve the problem of hypoxia-induced resistance to SDT and produce higher ROS to kill contractile hypoxia pancreatic cancer²⁰⁵. A nanoparticles consisting of methoxy-PEG-PCL (mPEG-PCL), IR780, PFOB, and CRGDK peptide-modified PEG-PCL could continuously supply O₂ to augment the sensitivity of tumor cells to PDT²⁰³. Zeolitic imidazolate framework-90 (ZIF-90) as an O₂ reservoir in nanoparticles could be degraded to quickly release O₂ at low pH, and the loaded RB could generate ROS under 808 nm, thus remarkably enhancing anti-tumor effects²⁰⁶. Biomimetic aggressive pseudo-RBCs composed of RBC membranes, hemoglobin (Hb), PDA, and MB could increase O₂ supply from the Hb-carried O₂ to overcome tumor hypoxia and impose strong PDT efficacy²⁰⁷.

Paclitaxel (PTX)/ICG and O₂-carrying liquid PFP co-loaded PLGA nanoparticles have been developed for PSDT/chemotherapy, which could supply O₂ to improve tumor hypoxia and exert anti-tumor effects against SKOV3 tumor¹⁴⁷.

4.6.4. Reducing endogenous O₂ consumption

NDDSs could be designed to reduce the endogenous O₂ consumption, thus efficiently attenuating the intratumoral hypoxia status. Tamoxifen in the nanocomplexes HSA-Ce6/tamoxifen could reduce the endogenous O₂ consumption under PDT process by inhibiting the activity of NADH dehydrogenase in the mitochondrial electron transport chain, thus greatly improving PDT treatment¹⁴⁰. Metformin can inhibit mitochondria-mediated respiration. PEG-PCL co-loaded with IR780 and metformin was developed to overcome tumor hypoxia and achieve superior synergistic PDT/PTT efficacy with reduced O₂ consumption. The tumor volume was inhibited by about 2.4-fold when the nanoparticles were exposed to laser irradiation²⁰⁸.

4.6.5. Promoting tumor blood flow

NDDSs can relieve tumor hypoxia through the promotion of tumor blood flow. Nitrosoglutathione (GSNO)- and Ce6-loaded zeolite imidazole framework-8 (ZIF-8) was coated with 4T1 cell membrane to fabricate biomimetic nanoplateform for SDT/gas therapy. Due to the thermal effect caused by ultrasound, the nanoplateform can promote tumor blood flow, thereby alleviating tumor hypoxia²⁰⁹. Poly (2-methacryloyloxyethyl phosphorylcholine) (PEG-*b*-PMPC) block copolymer, α-cyclodextrin (α-CD)-conjugated *S*-nitrosothiol (α-CD-NO), and α-CD-conjugated Ce6 were mixed together to form supramolecular nanoparticles α-CD-Ce6-NO. The α-CD-Ce6-NO could not only deplete intracellular GSH, but also relieve hypoxia at tumor sites through NO-mediated relaxation of smooth muscle cells (SMCs) and promotion of tumor blood flow. The subsequent generation of NO and ROS could react

with each other to generate reactive peroxynitrite (ONOO[−]) for enhanced PDT²¹⁰ (Fig. 6).

4.7. Employing different therapeutic modalities

Single-modality treatment is generally unable to obtain satisfactory effects due to the physiological complexity of tumors. Combination therapy can be introduced to target different mechanisms and inhibit different pathways, thereby improving the anti-cancer efficacy. PDT/SDT can be used in combination with other therapies for cancer treatment, such as chemotherapy, immunotherapy, and gene therapy^{25,211}. NDDSs can simultaneously deliver sensitizers and other drugs to achieve the synergistic SPDT and other therapies. Hollow mesoporous organosilica based nanosystems were used to carry PpIX and DOX to exert synergistic SDT/chemotherapeutic effects for hepatocellular carcinoma treatment²¹². TiO₂ nanocrystals coated with an O₂-deficient TiO_{2-x} layer were decorated with PEG in the outer layer. The nanocomposites demonstrated high photothermal conversion efficiency and high therapeutic biosafety for enhanced synergistic photothermal hyperthermia/SDT. The tumor suppression rate reached 100% in the combination group, which was higher than that in the group treated with only laser (54.2%) or only ultrasound (74.6%)²¹³. Bovine serum albumin (BSA) co-loaded with DOX and ICG can efficiently inhibit tumor growth through the integration of PDT and PTT with chemotherapy²¹⁴.

Peptide amphiphile C₁₈GR₇RGDS corporated with ICG could self-assemble into functional nanomicelles for *in vivo* PSDT/PTT combination therapy¹⁴⁴. PLGA loaded with PFP, ICG, and OXP have been developed for PSDT/chemotherapy¹⁹². PLGA carrying PTX and ICG could induce apoptosis of SKOV3 cells and inhibit SKOV3 tumor growth after PSDT/chemotherapy treatments¹⁴⁷.

4.8. Combining diagnosis and treatment

Cancer nanotheranostics involve the integration of diagnosis and treatment in a single plateform, which can monitor drug distribution and evaluate drug efficacy to adjust drug dosage and dosing regimen in time for precise cancer therapy²¹⁵. With the development of molecular imaging technology, various imaging modalities with different resolutions and sensitivities have been developed, including optical imaging, magnetic resonance imaging (MRI), computed topography (CT), positron emission tomography (PET), PA imaging, optical imaging, and ultrasound imaging²¹⁶. Nanoparticles carrying both sensitizers and imaging agents in one formulation could be used for simultaneous disease diagnosis and therapy. In addition, inorganic sensitizers themselves could be used as theranostic agents, such as noble metal nanoparticles (Au or Ag) for optical imaging, semiconductor nanoparticles (QD) for fluorescence imaging, and PHF for photoacoustic imaging²¹⁷.

ICG-loaded MSN was lidded with ZnO QDs and wrapped with erlotinib-modified chitosan to form a nanotheranostic system, which could activate the fluorescence recovery of ICG to identify different molecular subtypes of non-small cell lung cancer (NSCLC) cells though NIR fluorescence imaging and obtain PDT effects to reverse the resistance of NSCLC cells to molecular targeted drugs²¹⁸. Mn²⁺-chelated DVDMS was encapsulated into liposomes to form DVDMS-Mn-Liposomes for SDT. The nanoplateform could be used for *in vivo* monitoring of the drug bio-distribution and the tumor-growth suppression by fluorescence imaging and T1-weighted MRI²¹⁹.

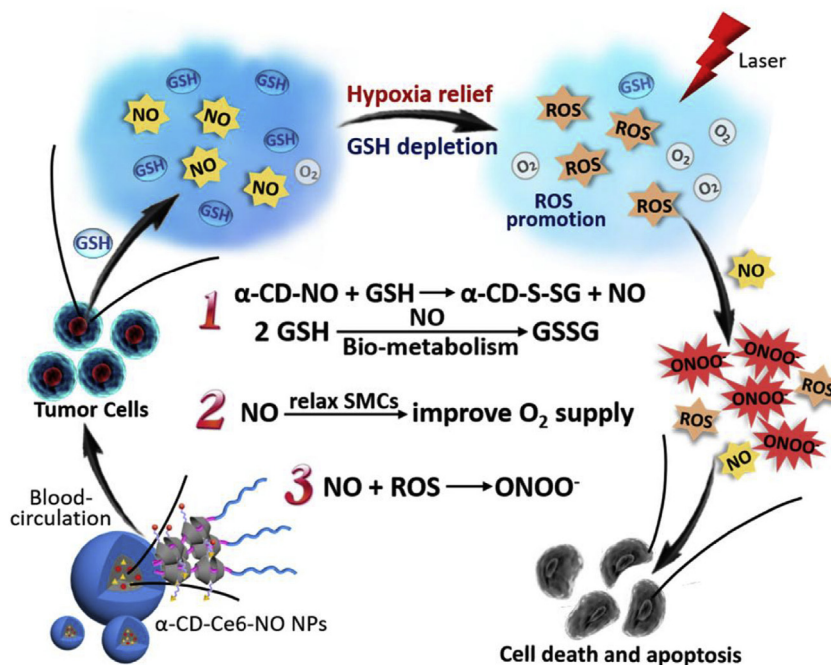


Figure 6 The schematic illustration of how the supramolecular nanoparticles α -CD-Ce6-NO improved the therapeutic efficacy. The α -CD-Ce6-NO could relieve hypoxia at tumor sites through NO-mediated relaxation of smooth muscle cells (SMCs) and promotion of tumor blood flow. Reprinted with the permission from Ref. 210. Copyright © 2018, Elsevier, Ltd.

FA-targeted PFH/ICG-loaded lipid nanoparticles have been developed for synergistic PSDT/PTT in ovarian cancer. The lipid nanoparticles could monitor the accumulation of drugs at the tumor region and be capable of enhancing the ultrasound/PA imaging with laser irradiation¹⁴². FA-conjugated lipid-polymer hybrid nanoparticles with core-shell structures were used to encapsulate ICG and perfluorocarbon (PFC)-carrying O₂ to construct a nanotheranostic agent. The nanotheranostic agent could not only generate large amounts of microbubbles to provide an excellent contrast for both PA and ultrasound imaging, but also generate ROS to achieve therapeutic effects upon PSDT treatments²²⁰.

5. Clinical application against cancer

In clinical research, PDT has been widely used to treat cancers. Because of the limited penetrability of light, PDT is usually used to treat superficial skin cancers. With the development of light source equipment, laser light can be transferred through fiber optic cables which could reach internal organs or cavities. Therefore, PDT has been used to treat cancer in the lungs or esophagus inside the body. According to the characteristics and types of tumors, PDT can exert its therapeutic effect alone, or can combine with surgery or other therapies^{221,222}. Patients treated with PDT could effectively improve clinical symptoms, reduce complications and improve quality of life. Adverse reactions in patients including skin solar sensitivity, pain in the irradiation area, and vocal cord edema and adhesion were reported^{223,224}. Some studies have shown that sensitizers can also be used for clinical diagnosis and treatment^{225,226}. PDT is usually used in combination with other therapies in clinic. Compared with surgery alone, patients with extramammary Paget's disease receiving 20% 5-ALA gel-mediated PDT combined with surgery could reduce recurrence

rate from 25% to 9.1%²²⁷. No recurrence was observed in two patients with recurrent and wide spread extramammary Paget disease underwent 20% 5-ALA gel and imiquimod combination treatment at 24- and 36-month follow-up²²⁸. Due to the restriction of the light, PDT is difficult to treat large tumors or cancer that has spread.

There are few studies on the clinical application of SDT and SPDT, and most of them are in the stage of cell or animal experiments. A 55-year-old patient with advanced breast cancer treated with immunotherapy (Gc protein-derived macrophage activating factor, GcMAF), SDT (Ce6 and 5-ALA) and hormone therapy (exemestane) showed dramatic improvement of symptoms (such as cough, back pain, and edema of the right hand) and the axillary tumors decreased and disappeared completely²²⁹. Preliminary clinical data revealed that sublingual administration of SF1 in 3 advanced refractory breast cancer patients treated with SPDT had significant partial or complete responses⁸¹. Another clinical outcome showed that numerous cases of the 115 patients treated with sonnelux-1-mediated SPDT had a significantly longer predicted median survival²³⁰. The main side effect of SPDT is pain or visible inflammatory reaction.

Although SPDT has been used in clinic and is available in several countries including England, Mexico, Israel, China, and Cape Town, there are still many problems that restricted its broad clinical applications. It still lacks sensitizers that are more effective, more selective, and are activated by both light and ultrasound. In addition, the deteriorating tumor microenvironment caused by SPDT can reduce the therapeutic effects. Moreover, there is few work on the development of systemic equipments for the delivery of light and generation of ultrasound that are convenient for clinical use. Furthermore, it is difficult to develop SPDT protocols that are suitable for clinical use.

Table 3 The advantages and disadvantages of organic, inorganic, and hybrid sensitizers.

Category	Advantage	Disadvantage
Organic sensitizers	<ul style="list-style-type: none"> • High selectivity • Low toxicity 	<ul style="list-style-type: none"> • Low water solubility • Limited light penetration • Chemical/biological instability • Skin phototoxicity • Aggregation in aqueous solutions • Poor pharmacokinetic behavior • Dose-dependent toxicity • Unsatisfactory ultrasound absorption coefficient • Lack of in-depth toxicological assessment
Inorganic sensitizers	<ul style="list-style-type: none"> • Good biocompatibility • Biological stability • NIR-II phototherapy • Multi-functionality 	
Hybrid sensitizers	<ul style="list-style-type: none"> • Combination of the unique properties of organic and inorganic sensitizers 	<ul style="list-style-type: none"> • Complex preparation procedures • Lack of detailed research

6. Conclusions and outlook

SPDT provides a highly promising approach to overcome the challenges and offer alternative opportunities in current anti-cancer fields. The development of new potential sensitizers is one of the most essential factors in SPDT. In this review, we attempted to provide an overview of sono/photosensitizers that can be developed into suitable sono-photosensitizers for SPDT and guide the design of the sensitizers. Sensitizers can be classified into organic, inorganic, and hybrid sensitizers. Each class has its own strengths and disadvantages (Table 3). Organic sensitizers generally have low toxicity, but poor water solubility and the chemical/biological instability limit their applications. Inorganic sensitizers are more stable than organic sensitizers, and some of the inorganic sensitizers can be designed for NIR-II phototherapy. However, they show relatively high toxicity and lack in-depth toxicological assessment. Although hybrid sensitizers can combine the advantages of organic and inorganic sensitizers, they are short of detailed and comprehensive researches²³¹. In addition, different types of sensitizers have different mechanisms of action. For example, organic sensitizers, such as ICG and Ce6 can generate ${}^1\text{O}_2$ through energy transfer mechanism, while inorganic sensitizers, such as Ag_2S and Au nanoparticles are activated by light to generate electron–hole ($e^- - h^+$) pairs, and then generate ROS for PDT. However, there is no clear distinction among the mechanisms of different types of sensitizers activated by ultrasound.

Ideal SPDT agents should exhibit strong sensitive, nontoxic, and high tumor-homing ability without rendering toxic side effects to improve therapeutic efficacy. Recently, some amphiphilic sensitizers, such as ICG, RBDs have been found to have favorable pharmacological and pharmaceutical properties for cancers in SPDT. Therefore, they might be the promising starting points for further rational drug design and molecular structure optimization in many aspects. Today, many institutes adopt the design of sensitizers as their main endeavor, with the aim of executing effective strategies toward cancers. Because some of the most typical sensitizers for SPDT were found from photosensitizers or sono-sensitizers, sensitizers for PDT or SDT could be developed into suitable sono-photosensitizers. Another strategy is applying the existing synthesis techniques for the efficient functionalization of current sensitizers. Hybrid sensitizers that combine the distinct advantages of organic and inorganic sensitizers can be developed. Because the limited penetration of light can affect the therapeutic

effect of SPDT, sensitizers with innovative structures and some more advanced stimulation tools should be found to increase the depth of light penetration into tissues. Fluorescence resonance energy transfer (FRET) or X-ray excitation source can be beneficial for deep tissue therapy^{232,233}. NIR-II excitable sensitizers are highly desirable for SPDT to improve light penetration depth in biotissues^{234–236}. In addition, sensitizers with both imaging capabilities and therapeutic functions can be designed for better use in individualized cancer treatment.

Although significant progress has been made in developing SPDT, further improvements of this program through a series of critical preclinical steps are needed prior to their ultimate clinical use. More work is needed to be done before SPDT is accepted as an adjuvant or replacement method for traditional cancer treatment. The efficacy of SPDT is closely related to the sensitizer dose, light dose, ultrasound intensity, and the order of PDT and SDT. For example, different irradiation times were used for the same sensitizers under the same wavelength and power due to the different doses administered in the body^{140,167}. It requires a lot of in-depth and comprehensive research to develop an appropriate standard operation procedure. In addition, the selection of appropriate dosage form, as well as the precise dose and medication method should be considered to increase drug compliance. As SPDT is usually used in combination with other therapies, there is an urgent need to clarify the biological mechanisms of SPDT and the synergistic effects of SPDT with other therapies. At present, a large number of clinical trials have been carried out using PDT for the treatment of brain, skin, prostate, cervix, and peritoneal cavity tumors²³⁷. Additionally, extracorporeal photopheresis (ECP) in which blood is treated with PDT *ex vivo* has been approved by FDA for patients with cutaneous T cell lymphoma (CTCL)²³⁸. Based on the results and the considerable experience gained from the clinical PDT studies, SPDT can be developed further and is expected to be a powerful tool used alone or in combination with other therapies against local or metastasis cancers.

NDDSS have achieved good results in cancer treatment and can be used to improve the anti-tumor effects of sensitizers. Some NDDSS with rational design are capable of crossing biological barriers into tumor sites. Ligands-modified NDDSS can actively target tumor blood vessels, tumor tissues/cells, and even cellular organelles, increasing cellular uptake and intracellular drugs concentration. Through size transition, charge reversal, or

membrane transport, sensitizers in NDDSs can penetrate into the internal area of the tumor and reach intratumoral cancer cells, thus improving the intratumoral delivery of sensitizers. NDDSs with stimuli-responsive release pattern could prevent premature leakage of sensitizers before reaching cancer cells, thus increasing the intracellular drugs concentration. Sensitizers-loaded NDDSs can be designed to stimulate anti-tumor immunity to prevent tumor metastasis and recurrence and to supply O₂ to alleviate tumor hypoxia, thereby enhancing the therapeutic effects. Combination therapies based on NDDSs can inhibit multiple pathways for enhanced SPDT. NDDSs that combine anti-cancer therapeutics with imaging modalities can be used for monitoring drug action sites and therapeutic response to change treatment strategies in time.

Besides the above-mentioned strategies that can be used to improve the anti-tumor SPDT effects of sensitizers, NDDSs can be further designed to provide more functionalities. Some sensitizers have short half-life and retention time in the body, and many sensitizers form aggregates in aqueous media due to π–π stacking, which can decrease or inhibit ¹O₂ generation, thus reducing the efficacy. NDDSs can be designed to prolong blood circulation time and prevent the aggregation of sensitizers for enhanced SPDT. The controlled release and activated imaging characteristics based on NDDSs can be designed for more precise SPDT. The combination of SPDT with PTT or chemotherapy has shown enhanced anti-tumor effects. NDDSs could provide a platform for combination of SPDT with other therapies, such as molecular targeted therapy, hyperthermia, gas therapy, gene therapy, and immunotherapy for more efficient cancer therapy. As mentioned above, the process of tumor drug delivery is very complicated, including at least five steps. Existing strategies can only improve one or two steps in CAPIR cascade, and cannot improve the overall transportation efficiency. NDDSs that could efficiently accomplish the full CAPIR cascade could be used to deliver sensitizers for SPDT to ensure the overall therapeutic efficiency.

Although NDDSs have made great progress in preclinical research, only a few have gone through feasible clinical trials. Excipientability and scale-up ability of NDDSs are two important factors restrict their clinical transformation. Design of NDDSs which could be prepared by a simple and mass-produced method is an essential prerequisite for further advancement of clinical research. There are few studies on the long-term toxicity and genotoxicity of various nanomaterials. Introducing interdisciplinary science to systematically study the biological safety of nanomaterials might accelerate the clinical conversion of NDDSs.

Acknowledgments

This work was supported by the National Natural Science Foundation of China (81871481 and 81571802), the Fujian Provincial Youth Top-notch Talent Support program (China), and National Key R&D Program of China (2020YFA0210800).

Author contributions

Yilin Zheng and Jinxiang Ye searched references and wrote the manuscript. Ziyi Li was in charge of drawing figures and sorting tables. Yu Gao and Haijun Chen revised the manuscript. All of the authors have read and approved the final manuscript.

Conflicts of interest

The authors have no conflicts of interest to declare.

Appendix A. Supporting information

Supporting data to this article can be found online at <https://doi.org/10.1016/j.apsb.2020.12.016>.

References

1. Siegel RL, Miller KD, Jemal A. Cancer statistics, 2017. *CA Cancer J Clin* 2017;**67**:7–30.
2. Dy GK, Adjei AA. Understanding, recognizing, and managing toxicities of targeted anticancer therapies. *CA Cancer J Clin* 2013;**63**:249–79.
3. Jiang YY, Li JC, Zeng ZL, Xie C, Lyu Y, Pu KY. Organic photodynamic nanoinhibitor for synergistic cancer therapy. *Angew Chem Int Ed Engl* 2019;**58**:8161–5.
4. Li JC, Huang JG, Lyu Y, Huang JS, Jiang YY, Xie C, et al. Photoactivatable organic semiconducting pro-nanoenzymes. *J Am Chem Soc* 2019;**141**:4073–9.
5. Ng CW, Li JC, Pu KY. Recent progresses in phototherapy-synergized cancer immunotherapy. *Adv Funct Mater* 2018;**28**:1804688.
6. Li JC, Cui D, Huang JG, He SS, Yang ZB, Zhang Y, et al. Organic semiconducting pro-nanostimulants for near-infrared photoactivatable cancer immunotherapy. *Angew Chem Int Ed Engl* 2019;**58**:12680–7.
7. Li JC, Luo Y, Pu KY. Electromagnetic nanomedicines for combinational cancer immunotherapy. *Angew Chem Int Ed Engl* 2020;**59**:11717.
8. Yin H, Kauffman KJ, Anderson DG. Delivery technologies for genome editing. *Nat Rev Drug Discov* 2017;**16**:387–99.
9. Chen HJ, Zhou XB, Gao Y, Zheng BY, Tang FX, Huang JD. Recent progress in development of new sonosensitizers for sonodynamic cancer therapy. *Drug Discov Today* 2014;**19**:502–9.
10. Yang YY, Tu J, Yang DX, Raymond JL, Roy RA, Zhang D. Photo- and sono-dynamic therapy: a review of mechanisms and considerations for pharmacological agents used in therapy incorporating light and sound. *Curr Pharmaceut Des* 2019;**25**:401–12.
11. Rai P, Mallidi S, Zheng X, Rahmazadeh R, Mir Y, Elrington S, et al. Development and applications of photo-triggered theranostic agents. *Adv Drug Deliv Rev* 2010;**62**:1094–124.
12. Lucky SS, Soo KC, Zhang Y. Nanoparticles in photodynamic therapy. *Chem Rev* 2015;**115**:1990–2042.
13. Gao Y, Xie JJ, Chen HJ, Gu SG, Zhao RL, Shao JW, et al. Nano-technology-based intelligent drug design for cancer metastasis treatment. *Biotechnol Adv* 2014;**32**:761–77.
14. Peng FF, Li RR, Zhang F, Qin L, Ling GX, Zhang P. Potential drug delivery nanosystems for improving tumor penetration. *Eur J Pharm Biopharm* 2020;**151**:220–38.
15. Zheng YL, Li ZY, Chen HJ, Gao Y. Nanoparticle-based drug delivery systems for controllable photodynamic cancer therapy. *Eur J Pharmaceut Sci* 2020;**144**:105213.
16. Li C, Wang JC, Wang YG, Gao HL, Wei G, Huang YZ, et al. Recent progress in drug delivery. *Acta Pharm Sin B* 2019;**9**:1145–62.
17. Luo ZJ, Dai Y, Gao HL. Development and application of hyaluronic acid in tumor targeting drug delivery. *Acta Pharm Sin B* 2019;**9**:1099–112.
18. Zhang B, Hu Y, Pang ZQ. Modulating the tumor microenvironment to enhance tumor nanomedicine delivery. *Front Pharmacol* 2017;**8**:952.
19. Foote CS. Definition of type I and type II photosensitized oxidation. *Photochem Photobiol* 1991;**54**:659.
20. Wang YY, Liu YC, Sun HW, Guo DS. Type I photodynamic therapy by organic–inorganic hybrid materials: from strategies to applications. *Coord Chem Rev* 2019;**395**:46–62.

21. Zhang J, Jiang CS, Figueiro Longo JP, Azevedo RB, Zhang H, Muehlmann LA. An updated overview on the development of new photosensitizers for anticancer photodynamic therapy. *Acta Pharm Sin B* 2018;**8**:137–46.
22. Allison RR, Moghissi K. Photodynamic therapy (PDT): PDT mechanisms. *Clin Endosc* 2013;**46**:24–9.
23. Rosenthal I, Sostaric JZ, Riesz P. Sonodynamic therapy—a review of the synergistic effects of drugs and ultrasound. *Ultrason Sonochem* 2004;**11**:349–63.
24. Liu XH, Li S, Wang M, Dai ZJ. Current status and future perspectives of sonodynamic therapy and sonosensitizers. *Asian Pac J Cancer Prev* 2015;**16**:4489–92.
25. Pan XT, Wang HY, Wang S, Sun X, Wang LJ, Wang WW, et al. Sonodynamic therapy (SDT): a novel strategy for cancer nanotheranostics. *Sci China Life Sci* 2018;**61**:415–26.
26. Ebraheminia A, Mokhtari-Dizaji M, Toliat T. Dual frequency cavitation event sensor with iodide dosimeter. *Ultrason Sonochem* 2016;**28**:276–82.
27. Pang X, Xu CS, Jiang Y, Xiao QC, Leung AW. Natural products in the discovery of novel sonosensitizers. *Pharmacol Ther* 2016;**162**:144–51.
28. Kolarova H, Bajgar R, Tomankova K, Krestyn E, Dolezal L, Halek J. *In vitro* study of reactive oxygen species production during photodynamic therapy in ultrasound-pretreated cancer cells. *Physiol Res* 2007;**56**:S27–32.
29. Jin ZH, Miyoshi N, Ishiguro K, Umemura S, Kawabata K, Yumita N, et al. Combination effect of photodynamic and sonodynamic therapy on experimental skin squamous cell carcinoma in C3H/HeN mice. *J Dermatol* 2000;**27**:294–306.
30. Li Q, Wang XB, Wang P, Zhang K, Wang HP, Feng XL, et al. Efficacy of chlorin e6-mediated sono-photodynamic therapy on 4T1 cells. *Cancer Biother Radiopharm* 2014;**29**:42–52.
31. Li Q, Liu QH, Wang P, Feng XL, Wang HP, Wang XB. The effects of Ce6-mediated sono-photodynamic therapy on cell migration, apoptosis and autophagy in mouse mammary 4T1 cell line. *Ultrasound* 2014;**54**:981–9.
32. Wang HP, Wang P, Zhang K, Wang XB, Liu QH. Changes in cell migration due to the combined effects of sonodynamic therapy and photodynamic therapy on MDA-MB-231 cells. *Laser Phys Lett* 2015;**12**:035603.
33. Liu QH, Wang XB, Wang P, Xiao LN, Hao Q. Comparison between sonodynamic effect with protoporphyrin IX and hematoporphyrin on sarcoma 180. *Cancer Chemother Pharmacol* 2007;**60**:671–80.
34. Kim J, Lim W, Kim S, Jeon S, Hui Z, Ni K, et al. Photodynamic therapy (PDT) resistance by PARP1 regulation on PDT-induced apoptosis with autophagy in head and neck cancer cells. *J Oral Pathol Med* 2014;**43**:675–84.
35. Hoi SW, Wong HM, Chan JY, Yue GG, Tse GM, Law BK, et al. Photodynamic therapy of pheophorbide a inhibits the proliferation of human breast tumour via both caspase-dependent and -independent apoptotic pathways in *in vitro* and *in vivo* models. *Phytother Res* 2012;**26**:734–42.
36. Umemura K, Yumita N, Nishigaki R, Umemura SI. Sonodynamically induced antitumor effect of pheophorbide a. *Cancer Lett* 1996;**102**:151–7.
37. Xu ZY, Wang K, Li XQ, Chen S, Deng JM, Cheng Y, et al. The ABCG2 transporter is a key molecular determinant of the efficacy of sonodynamic therapy with photofrin in glioma stem-like cells. *Ultrasound* 2013;**53**:232–8.
38. Qiu H, Kim MM, Penjweini R, Zhu TC. Macroscopic singlet oxygen modeling for dosimetry of photofrin-mediated photodynamic therapy: an *in-vivo* study. *J Biomed Optic* 2016;**21**:88002.
39. Li JH, Chen ZQ, Huang Z, Zhan Q, Ren FB, Liu JY, et al. *In vitro* study of low intensity ultrasound combined with different doses of PDT: effects on C6 glioma cells. *Oncol Lett* 2013;**5**:702–6.
40. Wang H, Wang XB, Wang P, Zhang K, Yang S, Liu QH. Ultrasound enhances the efficacy of chlorin e6-mediated photodynamic therapy in MDA-MB-231 cells. *Ultrasound Med Biol* 2013;**39**:1713–24.
41. Wang P, Li CF, Wang XB, Xiong WL, Feng XL, Liu QH, et al. Anti-metastatic and pro-apoptotic effects elicited by combination photodynamic therapy with sonodynamic therapy on breast cancer both *in vitro* and *in vivo*. *Ultrason Sonochem* 2015;**23**:116–27.
42. Tserkovsky DA, Alexandrova EN, Chalau VN, Istomin YP. Effects of combined sonodynamic and photodynamic therapies with photolon on a glioma C6 tumor model. *Exp Oncol* 2012;**34**:332–5.
43. Liu YC, Wang P, Liu QH, Wang XB. Sinoporphyrin sodium triggered sono-photodynamic effects on breast cancer both *in vitro* and *in vivo*. *Ultrason Sonochem* 2016;**31**:437–48.
44. Bakhshizadeh M, Moshirian T, Esmaily H, Rajabi O, Nassirli H, Sazgarnia A. Sonophotodynamic therapy mediated by liposomal zinc phthalocyanine in a colon carcinoma tumor model: role of irradiating arrangement. *Iran J Basic Med Sci* 2017;**20**:1088–92.
45. Tomankova K, Kolarova H, Kolar P, Kejlova K, Jirova D. Study of cytotoxic effect of photodynamically and sonodynamically activated sensitizers *in vitro*. *Toxicol Vitro* 2009;**23**:1465–71.
46. Tomankova K, Kolarova H, Bajgar R. Study of photodynamic and sonodynamic effect on A549 cell line by AFM and measurement of ROS production. *Phys Status Solidi* 2008;**205**:1472–7.
47. Chen HJ, Zhou XB, Wang AL, Zheng BY, Yeh CK, Huang JD. Synthesis and biological characterization of novel rose bengal derivatives with improved amphiphilicity for sono-photodynamic therapy. *Eur J Med Chem* 2018;**145**:86–95.
48. Nomikou N, Sterrett C, Arthur C, McCaughey B, Callan JF, McHale AP. The effects of ultrasound and light on indocyanine-green-treated tumour cells and tissues. *ChemMedChem* 2012;**7**:1465–71.
49. McEwan C, Nesbitt H, Nicholas D, Kavanagh ON, McKenna K, Loan P, et al. Comparing the efficacy of photodynamic and sono-dynamic therapy in non-melanoma and melanoma skin cancer. *Bioorg Med Chem* 2016;**24**:3023–8.
50. Shimamura Y, Tamatani D, Kuniyasu S, Mizuki Y, Suzuki T, Katsura H, et al. 5-aminolevulinic acid enhances ultrasound-mediated antitumor activity *via* mitochondrial oxidative damage in breast cancer. *Anticancer Res* 2016;**36**:3607–12.
51. He GF, Mu TL, Yuan YL, Yang WY, Zhang Y, Chen QY, et al. Effects of notch signaling pathway in cervical cancer by curcumin mediated photodynamic therapy and its possible mechanisms *in vitro* and *in vivo*. *J Cancer* 2019;**10**:4114–22.
52. Wang FP, Gao QP, Guo SY, Cheng JL, Sun X, Li QN, et al. The sonodynamic effect of curcumin on THP-1 cell-derived macrophages. *BioMed Res Int* 2013;**2013**:737264.
53. Petrellis MC, Frigo L, Ribeiro W, Leal-Junior EC, Oliveira FR, Maria DA, et al. Proinflammatory effects of photoactivated methylene blue on rat model of Walker 256 carcinosarcoma. *Exp Oncol* 2019;**41**:112–22.
54. Komori C, Okada K, Kawamura K, Chida S, Suzuki T. The sono-dynamic antitumor effect of methylene blue on sarcoma180 cells *in vitro*. *Anticancer Res* 2009;**29**:2411–5.
55. Ji YY, Ma YJ, Wang JW. Cytoprotective role of nitric oxide in HepG2 cell apoptosis induced by hypocrellin B photodynamic treatment. *J Photochem Photobiol, B* 2016;**163**:366–73.
56. Liu YC, Bai H, Wang HP, Wang XB, Liu QH, Zhang K, et al. Comparison of hypocrellin B-mediated sonodynamic responsiveness between sensitive and multidrug-resistant human gastric cancer cell lines. *J Med Ultrason* 2019;**46**:15–26.
57. Xiao L, Gu L, Howell SB, Sailor MJ. Porous silicon nanoparticle photosensitizers for singlet oxygen and their phototoxicity against cancer cells. *ACS Nano* 2011;**5**:3651–9.
58. Sviridov AP, Osminkina LA, Nikolaev AL, Kudryavtsev AA, Vasiliev AN, Timoshenko VY. Lowering of the cavitation threshold in aqueous suspensions of porous silicon nanoparticles for sonodynamic therapy applications. *Appl Phys Lett* 2015;**107**:123107.
59. Wang C, Cao SQ, Tie XX, Qiu B, Wu AH, Zheng ZH. Induction of cytotoxicity by photoexcitation of TiO₂ can prolong survival in glioma-bearing mice. *Mol Biol Rep* 2011;**38**:523–30.

60. Harada Y, Ogawa K, Irie Y, Endo H, Feril Jr LB, Uemura T, et al. Ultrasound activation of TiO_2 in melanoma tumors. *J Control Release* 2011;149:190–5.
61. Li C, Yang XQ, An J, Cheng K, Hou XL, Zhang XS, et al. Red blood cell membrane-enveloped O_2 self-supplementing biomimetic nanoparticles for tumor imaging-guided enhanced sonodynamic therapy. *Theranostics* 2020;10:867–9.
62. Cheng K, Zhang XS, An J, Li C, Zhang RY, Ye R, et al. Hitherto-unexplored photodynamic therapy of Ag_2S and enhanced regulation based on polydopamine *in vitro* and *vivo*. *Chemistry* 2019;25: 7553–60.
63. Bernard V, Mornstein V, Jaros J, Sedlackova M, Skorpikova J. Combined effect of silver nanoparticles and therapeutic ultrasound on ovarian carcinoma cells A2780. *J Appl Biomed* 2014;12:137–45.
64. Erdogan O, Abbak M, Demirbolat GM, Birtekocak F, Aksel M, Pasa S, et al. Green synthesis of silver nanoparticles via *Cynara scolymus* leaf extracts: the characterization, anticancer potential with photodynamic therapy in MCF7 cells. *PLoS One* 2019;14:e0216496.
65. Sazgarnia A, Shafei A, Taheri AR, Meibodi NT, Eshghi H, Attaran N, et al. Therapeutic effects of acoustic cavitation in the presence of gold nanoparticles on a colon tumor model. *J Ultrasound Med* 2013;32:475–83.
66. Wang H, Yang XZ, Shao W, Chen SC, Xie JF, Zhang XD, et al. Ultrathin black phosphorus nanosheets for efficient singlet oxygen generation. *J Am Chem Soc* 2015;137:11376–82.
67. Li ZY, Zhang TM, Fan F, Gao F, Ji HX, Yang LH. Piezoelectric materials as sonodynamic sensitizers to safely ablate tumors: a case study using black phosphorus. *J Phys Chem Lett* 2020;11:1228–38.
68. Berg K, Selbo PK, Weyergang A, Dietze A, Prasmickaita L, Bonsted A, et al. Porphyrin-related photosensitizers for cancer imaging and therapeutic applications. *J Microsc* 2005;218:133–47.
69. O'Connor AE, Gallagher WM, Byrne AT. Porphyrin and nonporphyrin photosensitizers in oncology: preclinical and clinical advances in photodynamic therapy. *Photochem Photobiol* 2009;85:1053–74.
70. Yao YH, Li J, Yuan LF, Zhang ZQ, Zhang FX. Novel porphyrin-Schiff base conjugates: synthesis, characterization and *in vitro* photodynamic activities. *RSC Adv* 2016;6:45681–8.
71. Liang S, Deng XR, Chang Y, Sun CQ, Shao S, Xie ZX, et al. Intelligent hollow Pt–CuS Janus architecture for synergistic catalysis-enhanced sonodynamic and photothermal cancer therapy. *Nano Lett* 2019;19:4134–45.
72. Musser DA, Datta-Gupta N. Inability to elicit rapid cytoidal effects on L1210 cells derived from porphyrin-injected mice following *in vitro* photoirradiation. *J Natl Cancer Inst* 1984;72:427–34.
73. Li GZ, Wang SP, Deng DS, Xiao ZS, Dong ZL, Wang ZP, et al. Fluorinated chitosan to enhance transmucosal delivery of sonosensitizer-conjugated catalase for sonodynamic bladder cancer treatment post-intravesical instillation. *ACS Nano* 2020;14:1586–99.
74. Song K, Kong BH, Li L, Yang QF, Wei YQ, Qu X. Intraperitoneal photodynamic therapy for an ovarian cancer ascite model in Fischer 344 rat using hematoporphyrin monomethyl ether. *Cancer Sci* 2007;98:1959–64.
75. Li JH, Song DY, Xu YG, Huang Z, Yue W. *In vitro* study of hematoporphyrin monomethyl ether-mediated sonodynamic effects on C6 glioma cells. *Neurol Sci* 2008;29:229–35.
76. Li HT, Song XY, Yang C, Li Q, Tang D, Tian WR, et al. Effect of hematoporphyrin monomethyl ether-mediated PDT on the mitochondria of canine breast cancer cells. *Photodiagnosis Photodyn Ther* 2013;10:414–21.
77. Miyoshi N, Ishihara M, Ono K, et al. Relative yield of active oxygens produced by various sensitizers *in vitro*. In: Yagi K, Kondo M, Niki E, Yoshikawa T, editors. *Oxygen radicals*. Amsterdam: Elsevier Science Publishers; 1992. p. 15–8.
78. Yumita N, Sasaki K, Umemura S, Yukawa A, Nishigaki R. Sonodynamically induced antitumor effect of gallium–porphyrin complex by focused ultrasound on experimental kidney tumor. *Cancer Lett* 1997;112:79–86.
79. Sadanala KC, Chaturvedi PK, Seo YM, Kim JM, Jo YS, Lee YK, et al. Sono-photodynamic combination therapy: a review on sensitizers. *Anticancer Res* 2014;34:4657–64.
80. Gomaa I, Ali SE, El-Tayeb TA, Abdel-kader MH. Chlorophyll derivative mediated PDT versus methotrexate: an *in vitro* study using MCF-7 cells. *Photodiagnosis Photodyn Ther* 2012;9:362–8.
81. Wang XH, Zhang WM, Xu ZY, Luo YF, Mitchell D, Moss RW. Sonodynamic and photodynamic therapy in advanced breast carcinoma: a report of 3 cases. *Integr Cancer Ther* 2009;8:283–7.
82. Lewis TJ. Toxicity and cytopathogenic properties toward human melanoma cells of activated cancer therapeutics in zebra fish. *Integr Cancer Ther* 2010;9:84–92.
83. Wang XH, Lewis TJ, Mitchell D. The tumoricidal effect of sono-dynamic therapy (SDT) on S-180 sarcoma in mice. *Integr Cancer Ther* 2008;7:96–102.
84. Kenyon JN, Fuller RJ. Outcome measures following sonodynamic photodynamic therapy—a case series. *Curr Drug Ther* 2011;6:12–6.
85. Chin WW, Heng PW, Thong PS, Bhuvaneswari R, Hirt W, Kuenzel S, et al. Improved formulation of photosensitizer chlorin e6 polyvinylpyrrolidone for fluorescence diagnostic imaging and photodynamic therapy of human cancer. *Eur J Pharm Biopharm* 2008;69:1083–93.
86. Ali-Seyed M, Bhuvaneswari R, Soo KC, Olivo M. Photolon™—photosensitization induces apoptosis via ROS-mediated cross-talk between mitochondria and lysosomes. *Int J Oncol* 2011; 39:821–31.
87. Tserkovsky DA, Alexandrova EN, Istomin YP. Photolon enhancement of ultrasound cytotoxicity. *Exp Oncol* 2011;33:107–9.
88. Wang XB, Hu JM, Wang P, Zhang SL, Liu YC, Xiong WL, et al. Analysis of the *in vivo* and *in vitro* effects of photodynamic therapy on breast cancer by using a sensitizer, sinoporphyrin sodium. *Theranostics* 2015;5:772–86.
89. Bottari G, de la Torre G, Torres T. Phthalocyanine-nanocarbon ensembles: from discrete molecular and supramolecular systems to hybrid nanomaterials. *Acc Chem Res* 2015;48:900–10.
90. Roguin LP, Chiarante N, Vior MCG, Marino J. Zinc(II) phthalocyanines as photosensitizers for antitumor photodynamic therapy. *Int J Biochem Cell Biol* 2019;114:105575.
91. Milowska K, Gabryelak T. Synergistic effect of ultrasound and phthalocyanines on nucleated erythrocytes *in vitro*. *Ultrasound Med Biol* 2005;31:1707–12.
92. Kolarova H, Lenobel R, Kolar P, Strnad M. Sensitivity of different cell lines to phototoxic effect of disulfonated chloroaluminium phthalocyanine. *Toxicol Vitro* 2007;21:1304–6.
93. Sugita N, Kawabata KI, Sasaki K, Sakata I, Umemura S. Synthesis of amphiphilic derivatives of rose bengal and their tumor accumulation. *Bioconjugate Chem* 2007;18:866–73.
94. Gao Y, Li ZH, Wang CQ, You JL, Jin BY, Mo F, et al. Self-assembled chitosan/rose bengal derivative nanoparticles for targeted sonodynamic therapy: preparation and tumor accumulation. *RSC Adv* 2015; 5:17915–23.
95. Nomikou N, Fowley C, Byrne NM, McCaughey B, McHale AP, Callan JF. Microbubble-sonosensitiser conjugates as therapeutics in sonodynamic therapy. *Chem Commun* 2012;48:8332–4.
96. Newton AD, Predina JD, Corbett CJ, Frenzel-Sulyok LG, Xia L, Petersson EJ, et al. Optimization of second window indocyanine green for intraoperative near-infrared imaging of thoracic malignancy. *J Am Coll Surg* 2019;228:188–97.
97. Yuan L, Lin WY, Zheng KB, He LW, Huang WM. Far-red to near infrared analyte-responsive fluorescent probes based on organic fluorophore platforms for fluorescence imaging. *Chem Soc Rev* 2013; 42:622–61.
98. Ghareei S, Pourhajibagher M, Chiniforush N, Raoofian R, Hashemi M, Shahabi S, et al. Effect of photodynamic therapy based on indocyanine green on expression of apoptosis-related genes in human gingival fibroblast cells. *Photodiagnosis Photodyn Ther* 2017; 19:33–6.

99. Sagir T, Gencer S, Kemikli N, Abasiyanik MF, Isik S, Ozturk R. Photodynamic activities of protoporphyrin IX and its dopamine conjugate against cancer and bacterial cell viability. *Med Chem Res* 2012;21:4499–505.
100. Su XM, Wang XB, Zhang K, Yang S, Liu QH, Leung AW, et al. Sonodynamic therapy induces apoptosis of human leukemia HL-60 cells in the presence of protoporphyrin IX. *Gen Physiol Biophys* 2016;35:155–64.
101. Li YJ, Huang P, Jiang CL, Jia de X, Du XX, Zhou JH, et al. Sonodynamically induced anti-tumor effect of 5-aminolevulinic acid on pancreatic cancer cells. *Ultrasound Med Biol* 2014;40:2671–9.
102. Foglietta F, Canaparo R, Francovich A, Civera P, Serpe L. In vitro study of sonodynamic and photodynamic treatment on human cancer cell lines. *Clin Therapeut* 2013;35:51–2.
103. Xu XY, Meng X, Li S, Gan RY, Li Y, Li HB. Bioactivity, health benefits, and related molecular mechanisms of curcumin: current progress, challenges, and perspectives. *Nutrients* 2018;10:1553.
104. Anand P, Kunnumakkara AB, Newman RA, Aggarwal BB. Bioavailability of curcumin: problems and promises. *Mol Pharm* 2007;4:807–18.
105. Park K, Lee JH. Photosensitizer effect of curcumin on UVB-irradiated HaCat cells through activation of caspase pathways. *Oncol Rep* 2007;17:537–40.
106. Wang XN, Xia XS, Leung AW, Xiang JY, Jiang Y, Wang P, et al. Ultrasound induces cellular destruction of nasopharyngeal carcinoma cells in the presence of curcumin. *Ultrasonics* 2011;51:165–70.
107. Wang XN, Leung AW, Luo JM, Xu CS. TEM observation of ultrasound-induced mitophagy in nasopharyngeal carcinoma cells in the presence of curcumin. *Exp Ther Med* 2012;3:146–8.
108. Suzuki N, Okada K, Chida S, Komori C, Shimada Y, Suzuki T. Antitumor effect of acridine orange under ultrasonic irradiation *in vitro*. *Anticancer Res* 2007;27:4179–84.
109. Osman H, Elsayah D, Saadatzadeh MR, Pollok KE, Yocom S, Hattab EM, et al. Acridine orange as a novel photosensitizer for photodynamic therapy in glioblastoma. *World Neurosurgery* 2018;114:e1310–5.
110. Wang KK, Zhang YF, Wang J, Yuan AH, Sun MJ, Wu JH, et al. Self-assembled IR780-loaded transferrin nanoparticles as an imaging, targeting and PDT/PTT agent for cancer therapy. *Sci Rep* 2016;6:27421.
111. Li YK, Zhou QF, Deng ZT, Pan M, Liu X, Wu JR, et al. IR-780 dye as a sonosensitizer for sonodynamic therapy of breast tumor. *Sci Rep* 2016;6:25968.
112. Mroz P, Pawlak A, Satti M, Lee H, Wharton T, Gali H, et al. Functionalized fullerenes mediate photodynamic killing of cancer cells: type I versus Type II photochemical mechanism. *Free Radic Biol Med* 2007;43:711–9.
113. Bosi S, Da Ros T, Spalluto G, Prato M. Fullerene derivatives: an attractive tool for biological applications. *Eur J Med Chem* 2003;38:913–23.
114. Vilen B, Lekka M, Sienkiewicz A, Marcoux P, Kulik AJ, Kasas S, et al. Singlet oxygen (${}^1\Delta_g$)-mediated oxidation of cellular and sub-cellular components: ESR and AFM assays. *J Phys-condens Mat* 2005;17:S1471–82.
115. Yumita N, Iwase Y, Watanabe T, Nishi K, Kuwahara H, Shigeyama M, et al. Involvement of reactive oxygen species in the enhancement of membrane lipid peroxidation by sonodynamic therapy with functionalized fullerenes. *Anticancer Res* 2014;34:6481–7.
116. Yumita N, Iwase Y, Imaizumi T, Sakurazawa A, Kaya Y, Nishi K, et al. Sonodynamically-induced anticancer effects by functionalized fullerenes. *Anticancer Res* 2013;33:3145–51.
117. Cullis AG, Canham LT, Calcott PD. The structural and luminescence properties of porous silicon. *J Appl Phys* 1997;82:909–65.
118. Canham LT. Silicon quantum wire array fabrication by electrochemical and chemical dissolution of wafers. *Appl Phys Lett* 1990;57:1046–8.
119. Fujii M, Minobe S, Usui M, Hayashi S, Gross E, Diener J, et al. Generation of singlet oxygen at room temperature mediated by energy transfer from photoexcited porousSi. *Phys Rev B* 2004;70:85311–5.
120. Osminkina LA, Nikolaev AL, Sviridov AP, Andronova NV, Tamarov KP, Gongalsky MB, et al. Porous silicon nanoparticles as efficient sensitizers for sonodynamic therapy of cancer. *Microporous Mesoporous Mater* 2015;210:169–75.
121. Ninomiya K, Noda K, Ogino C, Kuroda SI, Shimizu N. Enhanced OH radical generation by dual-frequency ultrasound with TiO₂ nanoparticles: its application to targeted sonodynamic therapy. *Ultrason Sonochem* 2014;21:289–94.
122. Ninomiya K, Ogino C, Oshima S, Sonobe S, Kuroda SI, Shimizu N. Targeted sonodynamic therapy using protein-modified TiO₂ nanoparticles. *Ultrason Sonochem* 2012;19:607–14.
123. Moosavi Nejad S, Takahashi H, Hosseini H, Watanabe A, Endo H, Narihira K, et al. Acute effects of sono-activated photocatalytic titanium dioxide nanoparticles on oral squamous cell carcinoma. *Ultrason Sonochem* 2016;32:95–101.
124. You DG, Deepagan VG, Um W, Jeon S, Son S, Chang H, et al. ROS-generating TiO₂ nanoparticles for non-invasive sonodynamic therapy of cancer. *Sci Rep* 2016;6:23200.
125. Rasmussen JW, Martinez E, Louka P, Wingett DG. Zinc oxide nanoparticles for selective destruction of tumor cells and potential for drug delivery applications. *Expet Opin Drug Deliv* 2010;7:1063–77.
126. Zhang HJ, Shan YF, Dong LJ. A comparison of TiO₂ and ZnO nanoparticles as photosensitizers in photodynamic therapy for cancer. *J Biomed Nanotechnol* 2014;10:1450–7.
127. Vighetto V, Ancona A, Racca L, Limongi T, Troia A, Canavese G, et al. The synergistic effect of nanocrystals combined with ultrasound in the generation of reactive oxygen species for biomedical applications. *Front Bioeng Biotechnol* 2019;7:374.
128. Liu Y, Wang Y, Zhen WY, Wang YH, Zhang ST, Zhao Y, et al. Defect modified zinc oxide with augmenting sonodynamic reactive oxygen species generation. *Biomaterials* 2020;251:120075.
129. Kouhnavaud M, Ikeda S, Ludin NA, Ahmad Khairudin NB, Ghaffari BV, Mat-Teridi MA, et al. A review of semiconductor materials as sensitizers for quantum dot-sensitized solar cells. *Renew Sustain Energy Rev* 2014;37:397–407.
130. Shanmuganathan R, Karuppusamy I, Saravanan M, Muthukumar H, Ponnuchamy K, Ramkumar VS, et al. Synthesis of silver nanoparticles and their biomedical applications—a comprehensive review. *Curr Pharmaceut Des* 2019;25:2650–60.
131. Vankayala R, Lin CC, Kalluru P, Chiang CS, Hwang KC. Gold nanoshells-mediated bimodal photodynamic and photothermal cancer treatment using ultra-low doses of near infra-red light. *Biomaterials* 2014;35:5527–38.
132. Shanei A, Akbari-Zadeh H. Investigating the sonodynamic-radiosensitivity effect of gold nanoparticles on HeLa cervical cancer cells. *J Kor Med Sci* 2019;34: e243.
133. Ma L, Chen W, Schatte G, Wang W, Joly AG, Huang YN, et al. A new Cu–cysteamine complex: structure and optical properties. *J Mater Chem C* 2014;2:4239–46.
134. Pandey NK, Chudal L, Phan J, Lin LW, Johnson O, Xing MY, et al. A facile method for the synthesis of copper-cysteamine nanoparticles and study of ROS production for cancer treatment. *J Mater Chem B* 2019;7:6630–42.
135. Liu ZP, Xiong L, Ouyang GQ, Ma L, Sahi S, Wang KP, et al. Investigation of copper cysteamine nanoparticles as a new type of radiosensitizers for colorectal carcinoma treatment. *Sci Rep* 2017;7:9290.
136. Wang P, Wang X, Ma L, Sahi S, Li L, Wang XB, et al. Nano-sonosensitization by using copper-cysteamine nanoparticles augmented sonodynamic cancer treatment. *Part Part Syst Char* 2018;35:1700378.
137. Zhang YF, He LY, Wu J, Wang KK, Wang J, Dai WM, et al. Switchable PDT for reducing skin photosensitization by a NIR dye

- inducing self-assembled and photo-disassembled nanoparticles. *Biomaterials* 2016; **107**:23–32.
138. Yu WQ, He XQ, Yang ZH, Yang XT, Xiao W, Liu R, et al. Sequentially responsive biomimetic nanoparticles with optimal size in combination with checkpoint blockade for cascade synergistic treatment of breast cancer and lung metastasis. *Biomaterials* 2019; **217**:119309.
139. Bidkar AP, Sanpui P, Ghosh SS. Transferrin-conjugated red blood cell membrane-coated poly(lactic-*co*-glycolic acid) nanoparticles for the delivery of doxorubicin and methylene blue. *Acs Applied Nano Materials* 2020; **3**:3807–19.
140. Yang ZJ, Chen Q, Chen JW, Dong ZL, Zhang R, Liu JJ, et al. Tumor-pH-responsive dissociable albumin–tamoxifen nanocomplexes enabling efficient tumor penetration and hypoxia relief for enhanced cancer photodynamic therapy. *Small* 2018; **14**:e1803262.
141. Sun QH, Sun XR, Ma XP, Zhou ZX, Jin EL, Zhang B, et al. Integration of nanoassembly functions for an effective delivery cascade for cancer drugs. *Adv Mater* 2014; **26**:7615–21.
142. Liu YJ, Chen SN, Sun JC, Zhu SY, Chen CY, Xie W, et al. Folate-targeted and oxygen/indocyanine green-loaded lipid nanoparticles for dual-mode imaging and photo-sonodynamic/photothermal therapy of ovarian cancer *in vitro* and *in vivo*. *Mol Pharm* 2019; **16**:4104–20.
143. Liu Z, Li JP, Jiang Y, Wang DD. Multifunctional nanocapsules on a seesaw balancing sonodynamic and photodynamic therapies against superficial malignant tumors by effective immune-enhancement. *Biomaterials* 2019; **218**:119251.
144. Liu Z, Li JP, Chen WN, Liu L, Yu FF. Light and sound to trigger the Pandora's box against breast cancer: a combination strategy of sonodynamic, photodynamic and photothermal therapies. *Biomaterials* 2020; **232**:119685.
145. Feng QH, Zhang WX, Yang XM, Li YZ, Hao YW, Zhang HL, et al. pH/ultrasound dual-responsive gas generator for ultrasound imaging-guided therapeutic inertial cavitation and sonodynamic therapy. *Adv Healthc Mater* 2018; **7**:2192–659.
146. Zhang HJ, Zhang XG, Ren YP, Cao F, Hou L, Zhang ZZ. An *in situ* microenvironmental nano-regulator to inhibit the proliferation and metastasis of 4T1 tumor. *Theranostics* 2019; **9**:3580–94.
147. Chen SN, Liu YJ, Zhu SY, Chen CY, Xie W, Xiao LL, et al. Dual-mode imaging and therapeutic effects of drug-loaded phase-transition nanoparticles combined with near-infrared laser and low-intensity ultrasound on ovarian cancer. *Drug Deliv* 2018; **25**:1683–93.
148. Lee HM, Jeong YI, Kim DH, Kwak TW, Chung CW, Kim CH, et al. Ursodeoxycholic acid-conjugated chitosan for photodynamic treatment of HuCC-T1 human cholangiocarcinoma cells. *Int J Pharm* 2013; **454**:74–81.
149. Wang HP, Wang P, Li L, Zhang K, Wang XB, Liu QH. Microbubbles enhance the antitumor effects of sinoporphyrin sodium mediated sonodynamic therapy both *in vitro* and *in vivo*. *Int J Biol Sci* 2015; **11**:1401–9.
150. Sun Y, Wang HP, Wang P, Zhang K, Geng XR, Liu QH, et al. Tumor targeting DVDMs-nanoliposomes for an enhanced sonodynamic therapy of gliomas. *Biomater Sci* 2019; **7**:985–94.
151. Hou R, Liang XL, Li XD, Zhang X, Ma XT, Wang F. *In situ* conversion of rose bengal microbubbles into nanoparticles for ultrasound imaging guided sonodynamic therapy with enhanced antitumor efficacy. *Biomater Sci* 2020; **8**:2526–36.
152. Zhang L, Yi HJ, Song J, Huang J, Yang K, Tan B, et al. Mitochondria-targeted and ultrasound-activated nanodroplets for enhanced deep-penetration sonodynamic cancer therapy. *ACS Appl Mater Interfaces* 2019; **11**:9355–66.
153. Ren H, Liu JQ, Li YQ, Wang HR, Ge SZ, Yuan AH, et al. Oxygen self-enriched nanoparticles functionalized with erythrocyte membranes for long circulation and enhanced phototherapy. *Acta Biomater* 2017; **59**:269–82.
154. Wu JN, Han HJ, Jin Q, Li ZH, Li H, Ji J. Design and proof of programmed 5-aminolevulinic acid prodrug nanocarriers for targeted photodynamic cancer therapy. *ACS Appl Mater Interfaces* 2017; **9**:14596–605.
155. Hou WX, Xia FF, Alves CS, Qian XQ, Yang YM, Cui DX. MMP2-targeting and redox-responsive PEGylated chlorin e6 nanoparticles for cancer near-infrared imaging and photodynamic therapy. *ACS Appl Mater Interfaces* 2016; **8**:1447–57.
156. He JY, Li CC, Ding L, Huang YN, Yin XL, Zhang JF, et al. Tumor targeting strategies of smart fluorescent nanoparticles and their applications in cancer diagnosis and treatment. *Adv Mater* 2019; **31**:e1902409.
157. Huang J, Liu FQ, Han XX, Zhang L, Hu ZQ, Jiang QQ, et al. Nanosonosensitizers for highly efficient sonodynamic cancer theranostics. *Theranostics* 2018; **8**:6178–94.
158. Lin HC, Li WT, Madanayake TW, Tao C, Niu Q, Yan SQ, et al. Aptamer-guided upconversion nanoplateform for targeted drug delivery and near-infrared light-triggered photodynamic therapy. *J Biomater Appl* 2020; **34**:875–88.
159. Lucky SS, Idris NM, Huang K, Kim J, Li Z, Thong PS, et al. *In vivo* biocompatibility, biodistribution and therapeutic efficiency of titania coated upconversion nanoparticles for photodynamic therapy of solid oral cancers. *Theranostics* 2016; **6**:1844–65.
160. Yang LM, Gao P, Huang YL, Lu X, Chang Q, Pan W, et al. Boosting the photodynamic therapy efficiency with a mitochondria-targeted nanophotosensitizer. *Chin Chem Lett* 2019; **30**:1293–6.
161. Lin KC, Lin ZG, Li YJ, Zheng YS, Zhang D. Ultrasound-induced reactive oxygen species generation and mitochondria-specific damage by sonodynamic agent/metal ion-doped mesoporous silica. *RSC Adv* 2019; **9**:39924–31.
162. Wan GY, Cheng YY, Song J, Chen Q, Chen BW, Liu YY, et al. Nucleus-targeting near-infrared nanoparticles based on TAT peptide-conjugated IR780 for photo-chemotherapy of breast cancer. *Chem Eng J* 2020; **380**:122458.
163. Wu D, Zhao Z, Wang N, Zhang XR, Yan HH, Chen XQ, et al. Fluorescence imaging-guided multifunctional liposomes for tumor-specific phototherapy for laryngeal carcinoma. *Biomater Sci* 2020; **8**:3443–53.
164. Li YZ, Hao LQ, Liu F, Yin LX, Yan SJ, Zhao HY, et al. Cell penetrating peptide-modified nanoparticles for tumor targeted imaging and synergistic effect of sonodynamic/HIFU therapy. *Int J Nanomed* 2019; **14**:5875–94.
165. Tong HX, Du JW, Li H, Jin Q, Wang YX, Ji J. Programmed photosensitizer conjugated supramolecular nanocarriers with dual targeting ability for enhanced photodynamic therapy. *Chem Commun* 2016; **52**:11935–8 (Camb).
166. Yu WQ, Liu R, Zhou Y, Gao HL. Size-tunable strategies for a tumor targeted drug delivery system. *ACS Cent Sci* 2020; **6**:100–16.
167. Yang GB, Phua SZF, Lim WQ, Zhang R, Feng LZ, Liu GF, et al. A hypoxia-responsive albumin-based nanosystem for deep tumor penetration and excellent therapeutic efficacy. *Adv Mater* 2019; **31**:e1901513.
168. Wang KW, Tu YL, Yao W, Zong QY, Xiao X, Yang RM, et al. Size-switchable nanoparticles with self-destructive and tumor penetration characteristics for site-specific phototherapy of cancer. *ACS Appl Mater Interfaces* 2020; **12**:6933–43.
169. Yang HY, Jang MS, Li Y, Fu Y, Wu TP, Lee JH, et al. Hierarchical tumor acidity-responsive self-assembled magnetic nanotheranostics for bimodal bioimaging and photodynamic therapy. *J Control Release* 2019; **301**:157–65.
170. Yang GB, Xu LG, Xu J, Zhang R, Song GS, Chao Y, et al. Smart nanoreactors for pH-responsive tumor homing, mitochondria-targeting, and enhanced photodynamic-immunotherapy of cancer. *Nano Lett* 2018; **18**:2475–84.
171. Li YX, An HX, Wang XB, Wang P, Qu F, Jiao Y, et al. Ultrasound-triggered release of sinoporphyrin sodium from liposome-microbubble complexes and its enhanced sonodynamic toxicity in breast cancer. *Nano Research* 2017; **11**:1038–56.
172. Wang YZ, Wang C, Ding Y, Li J, Li M, Liang X, et al. Biomimetic HDL nanoparticle mediated tumor targeted delivery of indocyanine green for enhanced photodynamic therapy. *Colloids Surf B BioInterfaces* 2016; **148**:533–40.

173. Thakur NS, Patel G, Kushwah V, Jain S, Banerjee UC. Self-assembled gold nanoparticle–lipid nanocomposites for on-demand delivery, tumor accumulation, and combined photothermal–photodynamic therapy. *ACS Applied Bio Materials* 2018;2:349–61.
174. Li Q, Sun LH, Hou MM, Chen QB, Yang RH, Zhang L, et al. A phase-change material packaged within hollow copper sulfide nanoparticles carrying doxorubicin and chlorin e6 for fluorescence-guided trimodal therapy of cancer. *ACS Appl Mater Interfaces* 2019;11:417–29.
175. Cao HL, Zhong S, Wang QS, Chen C, Tian J, Zhang WA. Enhanced photodynamic therapy based on an amphiphilic branched copolymer with pendant vinyl groups for simultaneous GSH depletion and Ce6 release. *J Mater Chem B* 2020;8:478–83.
176. Zhang CN, Shi GN, Zhang JF, Niu J, Huang PS, Wang ZH, et al. Redox- and light-responsive alginate nanoparticles as effective drug carriers for combinational anticancer therapy. *Nanoscale* 2017;9:3304–14.
177. Hou WX, Zhao X, Qian XQ, Pan F, Zhang CL, Yang YM, et al. pH-sensitive Self-assembling nanoparticles for tumor near-infrared fluorescence imaging and chemo-photodynamic combination therapy. *Nanoscale* 2016;8:104–16.
178. Wang L, Hu YJ, Hao YW, Li L, Zheng CX, Zhao HJ, et al. Tumor-targeting core–shell structured nanoparticles for drug procedural controlled release and cancer sonodynamic combined therapy. *J Control Release* 2018;286:74–84.
179. Shen LY, Huang Y, Chen D, Qiu F, Ma C, Jin X, et al. pH-Responsive aerobic nanoparticles for effective photodynamic therapy. *Theranostics* 2017;7:4537–50.
180. Dong ZL, Feng LZ, Zhu WW, Sun XQ, Gao M, Zhao H, et al. CaCO₃ nanoparticles as an ultra-sensitive tumor-pH-responsive nanoplate-form enabling real-time drug release monitoring and cancer combination therapy. *Biomaterials* 2016;110:60–70.
181. Yan TS, He JM, Liu RM, Liu ZH, Cheng JJ. Chitosan capped pH-responsive hollow mesoporous silica nanoparticles for targeted chemo-photo combination therapy. *Carbohydr Polym* 2020;231:115706.
182. Ren Y, Wang RR, Liu Y, Guo H, Zhou X, Yuan XB, et al. A hematoporphyrin-based delivery system for drug resistance reversal and tumor ablation. *Biomaterials* 2014;35:2462–70.
183. Yadav P, Zhang C, Whittaker AK, Kailasam K, Shanavas A. Magnetic and photocatalytic curcumin bound carbon nitride nano hybrids for enhanced glioma cell death. *ACS Biomater Sci Eng* 2019;5:6590–601.
184. John JV, Chung CW, Johnson RP, Jeong YI, Chung KD, Kang DH, et al. Dual stimuli-responsive vesicular nanospheres fabricated by lipopolymer hybrids for tumor-targeted photodynamic therapy. *Biopolymers* 2016;17:20–31.
185. Jing XN, Zhi Z, Jin LM, Wang F, Wu YS, Wang DQ, et al. pH/redox dual-stimuli-responsive cross-linked polyphosphazene nanoparticles for multimodal imaging-guided chemo-photodynamic therapy. *Nanoscale* 2019;11:9457–67.
186. Chu CW, Ryu JH, Jeong YIL, Kwak TW, Lee HL, Kim HY, et al. Redox-responsive nanophotosensitizer composed of chlorin e6-conjugated dextran for photodynamic treatment of colon cancer cells. *J Nanomater* 2016;2016:1–12.
187. Li XD, Wang J, Cui RR, Xu DK, Zhu LS, Li ZY, et al. Hypoxia/pH dual-responsive nitroimidazole-modified chitosan/rose bengal derivative nanoparticles for enhanced photodynamic anticancer therapy. *Dyes Pigments* 2020;179:108395.
188. Zhang N, Zhao FF, Zou QL, Li YX, Ma GH, Yan XH. Multitargeted tumor-responsive drug delivery vehicles based on protein and peptide coassembly for enhanced photodynamic tumor ablation. *Small* 2016;12:5936–43.
189. Song WT, Musetti SN, Huang L. Nanomaterials for cancer immunotherapy. *Biomaterials* 2017;148:16–30.
190. Ding BB, Zheng P, Ma PA, Lin J. Manganese oxide nanomaterials: synthesis, properties, and theranostic applications. *Adv Mater* 2020;32:e1905823.
191. Mroz P, Hashmi JT, Huang YY, Lange N, Hamblin MR. Stimulation of anti-tumor immunity by photodynamic therapy. *Expt Rev Clin Immunol* 2011;7:75–91.
192. Xie W, Zhu S, Yang BY, Chen CY, Chen SN, Liu YJ, et al. The destruction of laser-induced phase-transition nanoparticles triggered by low-intensity ultrasound: an innovative modality to enhance the immunological treatment of ovarian cancer cells. *Int J Nanomed* 2019;14:9377–93.
193. Sentebane DA, Rowe A, Thomford NE, Shipanga H, Munro D, Mazeedi M, et al. The role of tumor microenvironment in chemoresistance: to survive, keep your enemies closer. *Int J Mol Sci* 2017;18:1586.
194. Kumari R, Sunil D, Ningthoujam RS. Hypoxia-responsive nanoparticle based drug delivery systems in cancer therapy: an up-to-date review. *J Control Release* 2020;319:135–56.
195. Li G, Yuan S, Deng D, Ou T, Li Y, Sun R, et al. Fluorinated polyethylenimine to enable transmucosal delivery of photosensitizer-conjugated catalase for photodynamic therapy of orthotopic bladder tumors postintravesical instillation. *Adv Funct Mater* 2019;29:1901932.
196. Wang TT, Zhang H, Han YB, Liu HH, Ren F, Zeng JF, et al. Light-enhanced O₂-evolving nanoparticles boost photodynamic therapy to elicit antitumor immunity. *ACS Appl Mater Interfaces* 2019;11:16367–79.
197. Wu X, Yan PJ, Ren ZH, Wang YF, Cai XJ, Li X, et al. Ferric hydroxide-modified upconversion nanoparticles for 808 nm NIR-triggered synergistic tumor therapy with hypoxia modulation. *ACS Appl Mater Interfaces* 2019;11:385–93.
198. Zhang Y, Xu YJ, Sun D, Meng ZY, Ying WW, Gao W, et al. Hollow magnetic nanosystem-boosting synergistic effect between magnetic hyperthermia and sonodynamic therapy via modulating reactive oxygen species and heat shock proteins. *Chem Eng J* 2020;390:124521.
199. Liu XM, Tian K, Zhang JH, Zhao ML, Liu SJ, Zhao Q, et al. Smart NIR-light-mediated nanotherapeutic agents for enhancing tumor accumulation and overcoming hypoxia in synergistic cancer therapy. *ACS Applied Bio Materials* 2019;2:1225–32.
200. Liang S, Deng XR, Xu GY, Xiao X, Wang MF, Guo XS, et al. A novel Pt-TiO₂ heterostructure with oxygen-deficient layer as bilaterally enhanced sonosensitizer for synergistic chemo-sonodynamic cancer therapy. *Adv Funct Mater* 2020;30:1908598.
201. Wang M, Chang MY, Chen Q, Wang DM, Li CX, Hou ZY, et al. Au₂Pt-PEG-Ce6 nanoformulation with dual nanzyme activities for synergistic chemodynamic therapy/phototherapy. *Biomaterials* 2020;252:120093.
202. Lin TS, Zhao XZ, Zhao S, Yu H, Cao WM, Chen W, et al. O₂-generating MnO₂ nanoparticles for enhanced photodynamic therapy of bladder cancer by ameliorating hypoxia. *Theranostics* 2018;8:990–1004.
203. Zhao CY, Tong YJ, Li XL, Shao LH, Chen L, Lu JQ, et al. Photosensitive nanoparticles combining vascular-independent intratumor distribution and on-demand oxygen-depot delivery for enhanced cancer photodynamic therapy. *Small* 2018;14:e1703045.
204. Wang HY, Hou L, Li HL, Wang X, Cao Y, Zhang BY, et al. A nanosystem loaded with perfluorohexane and rose bengal coupled upconversion nanoparticles for multimodal imaging and synergistic chemo-photodynamic therapy of cancer. *Biomater Sci* 2020;8:2488–506.
205. Chen J, Luo HL, Liu Y, Zhang W, Li HX, Luo T, et al. Oxygen-self-produced nanoplateform for relieving hypoxia and breaking resistance to sonodynamic treatment of pancreatic cancer. *ACS Nano* 2017;11:12849–62.
206. Xie ZX, Cai XC, Sun CQ, Liang S, Shao S, Huang SS, et al. O₂-loaded pH-responsive multifunctional nanodrug carrier for overcoming hypoxia and highly efficient chemo-photodynamic cancer therapy. *Chem Mater* 2018;31:483–90.
207. Liu WL, Liu T, Zou MZ, Yu WY, Li CX, He ZY, et al. Aggressive man-made red blood cells for hypoxia-resistant photodynamic therapy. *Adv Mater* 2018;30:e1802006.

208. Yang ZY, Wang JF, Liu S, Li XH, Miao LY, Yang B, et al. Defeating relapsed and refractory malignancies through a nano-enabled mitochondria-mediated respiratory inhibition and damage pathway. *Biomaterials* 2020;229:119580.
209. An J, Hu YG, Li C, Hou XL, Cheng K, Zhang B, et al. A pH/ultrasound dual-response biomimetic nanoplatform for nitric oxide gas-sonodynamic combined therapy and repeated ultrasound for relieving hypoxia. *Biomaterials* 2020;230:119636.
210. Deng YY, Jia F, Chen SY, Shen ZD, Jin Q, Fu GS, et al. Nitric oxide as an all-rounder for enhanced photodynamic therapy: hypoxia relief, glutathione depletion and reactive nitrogen species generation. *Biomaterials* 2018;187:55–65.
211. Brodin NP, Guha C, Tome WA. Photodynamic therapy and its role in combined modality anticancer treatment. *Technol Cancer Res Treat* 2015;14:355–68.
212. Li ZL, Han J, Yu LD, Qian XQ, Xing H, Lin H, et al. Synergistic sonodynamic/chemotherapeutic suppression of hepatocellular carcinoma by targeted biodegradable mesoporous nanosonosensitizers. *Adv Funct Mater* 2018;28:1800145.
213. Han XX, Huang J, Jing XX, Yang DY, Lin H, Wang ZG, et al. Oxygen-deficient black titania for synergistic/enhanced sonodynamic and photoinduced cancer therapy at near infrared-II biowindow. *ACS Nano* 2018;12:4545–55.
214. Xu L, Wang SB, Xu C, Han D, Ren XH, Zhang XZ, et al. Multi-functional albumin-based delivery system generated by programmed assembly for tumor-targeted multimodal therapy and imaging. *ACS Appl Mater Interfaces* 2019;11:38385–94.
215. Zheng YL, Gao Y. Molecular targeted nanotheranostics for future individualized cancer treatment. *Expert Opin Drug Deliv* 2020;17:1059–62.
216. Chen ZY, Wang YX, Lin Y, Zhang JS, Yang F, Zhou QL, et al. Advance of molecular imaging technology and targeted imaging agent in imaging and therapy. *BioMed Res Int* 2014;2014:819324.
217. Kievit FM, Zhang MQ. Cancer nanotheranostics: improving imaging and therapy by targeted delivery across biological barriers. *Adv Mater* 2011;23:H217–47.
218. Zhang YY, Zhang L, Lin XW, Ke LJ, Li BF, Xu L, et al. Dual-responsive nanosystem for precise molecular subtyping and resistant reversal of EGFR targeted therapy. *Chem Eng J* 2019;372:483–95.
219. Liu HM, Zhou MJ, Sheng ZH, Chen YK, Yeh CK, Chen WT, et al. Theranostic nanosensitizers for highly efficient MR/fluorescence imaging-guided sonodynamic therapy of gliomas. *J Cell Mol Med* 2018;22:5394–405.
220. Chen CY, Sun JC, Chen SN, Liu YJ, Zhu SY, Wang ZG, et al. A multifunctional-targeted nanoagent for dual-mode image-guided therapeutic effects on ovarian cancer cells. *Int J Nanomed* 2019;14:753–69.
221. Yano S, Hirohara S, Obata M, Hagiya Y, Ogura SI, Ikeda A, et al. Current states and future views in photodynamic therapy. *J Photochem Photobiol C Photochem Rev* 2011;12:46–67.
222. Lucena SR, Salazar N, Gracia-Cazana T, Zamarron A, Gonzalez S, Juarranz A, et al. Combined treatments with photodynamic therapy for non-melanoma skin cancer. *Int J Mol Sci* 2015;16:25912–33.
223. Sun BO, Li W, Liu N. Curative effect of the recent photofrin photodynamic adjuvant treatment on young patients with advanced colorectal cancer. *Oncol Lett* 2016;11:2071–4.
224. Hosokawa S, Takahashi G, Sugiyama KI, Takebayashi S, Okamura J, Takizawa Y, et al. Porfimer sodium-mediated photodynamic therapy in patients with head and neck squamous cell carcinoma. *Photodiagnosis Photodyn Ther* 2020;29:101627.
225. Papayan G, Goncharov S, Kazakov N, Strui A, Akopov A. Clinical potential of photodynamic diagnosis and therapy of tracheobronchial malignancies in the visible and infrared spectral ranges. *Translational Biophotonics* 2020;2:e201900019.
226. Farrakhova D, Shiryaev A, Yakovlev D, Efendiev K, Maklygina Y, Borodkin A, et al. Trials of a fluorescent endoscopic video system for diagnosis and treatment of the head and neck cancer. *J Clin Med* 2019;8:2229.
227. Wang HW, Lv T, Zhang LL, Lai YX, Tang L, Tang YC, et al. A prospective pilot study to evaluate combined topical photodynamic therapy and surgery for extramammary Paget's disease. *Laser Surg Med* 2013;45:296–301.
228. Jing W, Juan X, Li X, Chen JY, Qin H, Qing L, et al. Complete remission of two patients with recurrent and wide spread extramammary Paget disease obtained from 5-aminolevulinic acid-based photodynamic therapy and imiquimod combination treatment. *Photodiagnosis Photodyn Ther* 2014;11:434–40.
229. Inui T, Makita K, Miura H, Matsuda A, Kuchiike D, Kubo K, et al. Case report: a breast cancer patient treated with GcMAF, sonodynamic therapy and hormone therapy. *Anticancer Res* 2014;34:4589–93.
230. Kenyon JN, Fulle RJ, Lewis TJ. Activated cancer therapy using light and ultrasound—a case series of sonodynamic photodynamic therapy in 115 patients over a 4 year period. *Curr Drug Ther* 2009;4:179–93.
231. Lin XH, Song JB, Chen XY, Yang HH. Ultrasound activated sensitizers and applications. *Angew Chem Int Ed Engl* 2020;59:2–24.
232. Niu N, Zhang Z, Gao X, Chen ZJ, Li SJ, Li J. Photodynamic therapy in hypoxia: near-infrared-sensitive, self-supported, oxygen generation nano-platform enabled by upconverting nanoparticles. *Chem Eng J* 2018;352:818–27.
233. Hsu CC, Lin SL, Chang CA. Lanthanide-doped core–shell–shell nanocomposite for dual photodynamic therapy and luminescence imaging by a single X-ray excitation source. *ACS Appl Mater Interfaces* 2018;10:7859–70.
234. Jiang YY, Li JC, Zhen X, Xie C, Pu KY. Dual-peak absorbing semiconducting copolymer nanoparticles for first and second near-infrared window photothermal therapy: a comparative study. *Adv Mater* 2018;30:e1705980.
235. Jiang YY, Upputuri PK, Xie C, Zeng ZL, Sharma A, Zhen X, et al. Metabolizable semiconducting polymer nanoparticles for second near-infrared photoacoustic imaging. *Adv Mater* 2019;31:e1808166.
236. Jiang YY, Zhao XH, Huang JG, Li JC, Upputuri PK, Sun H, et al. Transformable hybrid semiconducting polymer nanzyme for second near-infrared photothermal ferrotherapy. *Nat Commun* 2020;11:1857.
237. Dos Santos AIF, De Almeida DRQ, Terra LF, Baptista MS, Labriola L. Photodynamic therapy in cancer treatment—an update review. *J Cancer Metastasis and Treatment* 2019;5:25.
238. Hannani D. Extracorporeal photopheresis: tolerogenic or immunogenic cell death? Beyond current dogma. *Front Immunol* 2015;6:349.